Received: 30 October 2020 | Revised: 21 October 2021 | Accepted: 25 October 2021

DOI: 10.1111/gbi.12480

ORIGINAL ARTICLE

gebiology WILEY

Comparative soft-tissue preservation in Holocene-age capelin concretions

Angel Mojarro[1] | Xingqian Cui[1] | Xiaowen Zhang[1] | Adam B. Jost[1] | Kristin D. Bergmann[1] | Jakob Vinther[2] | Roger E. Summons[1]

[1]Department of Earth, Atmospheric and Planetary Sciences, Massachusetts Institute of Technology, Cambridge, Massachusetts, USA

[2]School of Biological Sciences, University of Bristol, Bristol, UK

Correspondence
Angel Mojarro, Massachusetts Institute of Technology, 77 Massachusetts Ave, Room E25-647, Cambridge, MA 02139, USA.
Email: mojarro@mit.edu

Present address
Xingqian Cui and Xiaowen Zhang, School of Oceanography, Shanghai Jiao Tong University, Shanghai, China

Funding information
Dean of Science Fellowship, Massachusetts Institute of Technology; Office of Graduate Education, Massachusetts Institute of Technology; Simons Foundation

Abstract

Determining how soft tissues are preserved and persist through geologic time are continuing challenge because decay begins immediately after senescence while diagenetic transformations generally progress over days to millions of years. However, in recent years, carbonate concretions containing partially-to-fully decayed macroorganisms have proven to be remarkable windows into the diagenetic continuum revealing insights into the fossilization process. This is because most concretions are the result of biologically induced mineral precipitation caused by the localized decay of organic matter, which oftentimes preserves a greater biological signal relative to their host sediment. Here we present a comparative lipid biomarker study investigating processes associated with soft-tissue preservation within Holocene-age carbonate concretions that have encapsulated modern capelin (*Mallotus villosus*). We focus on samples collected from two depositional settings that have produced highly contrasting preservation end-members: (1) Kangerlussuaq, Greenland: a marine environment, which, due to isostatic rebound, has exposed strata containing concretions exhibiting exceptional soft-tissue preservation (6–7 kya), and (2) Greens Creek, Ottawa, Canada: a paleo brackish-to-freshwater marine excursion containing concretions exhibiting skeletal remains (~11 kya). Lipid biomarker analysis reveals endogenous capelin tissues and productive waters at Kangerlussuaq that are in sharp contrast to Greens Creek concretions, which lack appreciable capelin and environmental signals. Comparable distributions of bacterial fatty acids and statistical analyses suggest soft-tissue preservation within concretions is agnostic to specific heterotrophic decay communities. We, therefore, interpret preservation within carbonate concretions may represent a race between microbially induced authigenic precipitation and decay. Namely, factors resulting in exceptional preservation within concretions likely include: (1) organic matter input, (2) rate of decay, (3) carbonate saturation, (4) porewater velocity, and (5) rate of authigenic (carbonate) precipitation resulting in arrested decay/bacterial respiration due to cementing pore spaces limiting the diffusion of electron acceptors into the decay foci.

KEYWORDS
biomarkers, carbonate concretions, fossilization, soft-tissue preservation

1 | INTRODUCTION

Determining how animal fossils form and the ways in which their soft tissues are preserved in the geologic record has been a challenge to unravel because decay begins immediately after senescence while diagenetic alteration of organic matter continues over millions of years. Laboratory experiments running days to years provide important insights to some of the processes taking place (e.gAllison, 1986; Briggs & Kear, 1993; Butler et al., 2015; Darroch et al., 2012; Gäb et al., 2020; Gupta et al., 2009; Iniesto et al., 2013; McCoy et al., 2015b; Naimark et al., 2016; Sansom et al., 2011). However, fossilization is ultimately the consequence of compounding factors, and this complexity poses various challenges for laboratory and modeling studies (Briggs, 1995; Briggs & McMahon, 2016; Parry et al., 2018; Purnell et al., 2018; Sansom, 2014). Pathways of organic matter preservation are thought to not only depend on its original composition (e.g., Sansom et al., 2011), but also contingent on the depositional setting (e.g., sedimentation rates, sedimentary composition, water chemistry, etc.) (Allison, 1988a; Elder & Smith, 1988), and the nature of microorganisms involved in decay (Allison, 1988b; Briggs, 2003; Gäb et al., 2020; Iniesto et al., 2015, 2017). Therefore, while taphonomic experiments have significantly advanced our understanding of soft-tissue preservation, it would be ideal if fossilization could be caught in the act under natural conditions.

In recent years, with the application of contemporary organic geochemistry techniques (e.g., gas chromatography-mass spectrometry), interest surrounding carbonate concretions has seen a resurgence as potential windows into the fossilization process or the 'diagenetic continuum' (Melendez et al., 2013). Ubiquitous throughout the geological record, carbonate concretions are thought to be the result of biologically induced (i.e., Dupraz et al., 2009) authigenic precipitation containing a range of partially-to-fully decayed macroorganisms as their nucleus (Clements et al., 2019; Coleman, 1993; Duan et al., 1996; Raiswell, 1976; Zatoń & Marynowski, 2004). Although concretions without obvious organic foci have also been described (e.g., McBride & Milliken, 2006). Specifically, their formation has been proposed to be the result of (1) anaerobic microbial decay of an organic carbon source (e.g., a dead fish) resulting in (2) localized supersaturation of HCO_3^- ions, which generate a pH and alkalinity gradient (i.e., microenvironment) that is (3) proportional to the rate of decay and diffusion resulting in (4) the decreased solubility (i.e., increased saturation index) and consequent microbially induced carbonate precipitation (Berner, 1968, 1969; Coleman, 1993; Coleman & Raiswell, 1981, 1995; Mozley, 1996; Pye et al., 1990; Raiswell, 1976; Raiswell & Fisher, 2000).

Due to their frequent association with encapsulated organisms, concretions are particularly interesting for studying the fossilization of animal soft tissues (Thiel & Hoppert, 2018; Wilson & Brett, 2013). This is because authigenic mineral precipitation has been observed to entomb organic carbon sources within carbonate matrices ensuring its survival through diagenesis (Blumenberg et al., 2015; Brown et al., 2017; Grice et al., 2019; Mcnamara et al., 2009; Melendez, Grice, & Schwark, 2013; Plet et al., 2017). Moreover, organomineralized and biomineralized carbonates (e.g., stromatolites, eggshells, seashells, coccoliths) have been shown to adsorb and encapsulate peptide sequences, polysaccharides, DNA, and lipids for timescales beyond their normal stability range (Crisp et al., 2013; Demarchi et al., 2016; Oskam et al., 2010; Sand et al., 2014). Mineral precipitation may also fractionate biomarkers into inter- and intracrystalline species with varying degrees of diagenetic alteration (Ingalls et al., 2004). Therefore, carbonate concretions containing a discernable organic carbon source and low thermal maturity may be viewed as instances where the fossilization process has effectively been 'caught in the act' in its natural state (Thiel & Hoppert, 2018; Wilson & Brett, 2013). This notion is supported by work demonstrating concretions can preserve signals for the nucleating organism (Melendez, Grice, Trinajstic, et al., 2013), diagenesis (Melendez, Grice, & Schwark, 2013), and the sedimentary environment (Lengger et al., 2017; Thiel & Hoppert, 2018).

During the earliest steps of animal decay, autolysis by hydrolytic enzymes digest carbohydrates and proteins while labile organic compounds are quickly remineralized by heterotrophs (Butler et al., 2015; Gäb et al., 2020; Iniesto et al., 2017). Under aerobic conditions, these processes, along with bioturbation and scavenging, can result in the complete destruction of organic matter in sediments (Hedges & Keil, 1995; Lehmann et al., 2002; Sun et al., 1997). As the supply of oxygen is consumed by respiration, microorganisms then transition toward less-optimal terminal electron acceptors (e.g., SO_4^{2-}, Fe^{3+}), which effectively decrease rates of decay (Andersen, 1996; Muscente et al., 2017). However, this shift does not necessarily result in an increased preservation potential although anoxic conditions may restrict scavenging and permit the preservation of articulated body fossils under some settings (Allison, 1988a). Thereafter, recalcitrant materials (e.g., biomineralized tissue, lipids, and some polymers such as melanin) may survive due to selective preservation and/or diagenetic transformation into their stable counterparts and incorporations into macro polymers (Alleon et al., 2017; Briggs & Summons, 2014; Gupta et al., 2009; Larter & Douglas, 1980; Lindgren et al., 2012; Wiemann et al., 2018). Interestingly, taphonomic studies have suggested that communities responsible for decay may paradoxically be responsible for enhanced preservation (Allison, 1988b; Briggs, 2003; Darroch et al., 2012; Iniesto et al., 2013; Sagemann et al., 1999). For instance, sulfate-reducing bacteria (SRB) sustaining H_2S-rich conditions (i.e., euxinia) appear to have mediated the preservation of cholesterol and diagenetically modified derivatives for approximately 380 million years within a carbonate concretion (Melendez, Grice, Trinajstic, et al., 2013). This has been inferred to be via (1) authigenic carbonate precipitation and subsequent encapsulation (Raiswell & Fisher, 2000), (2) sulfurization of lipids (Adam et al., 2000), and (3) abiotic H_2S-mediated hydrogenation (Hebting, 2006).

Despite the advances in understanding preservation mechanisms within concretions, the nature of biological activity in more

recent settings affords an opportunity to identify biases relevant to the wider topic of animal soft-tissue and lipid biomarker preservation in the geological record. In this study, we investigate the role of biotic and abiotic mechanisms (e.g., decay, authigenic precipitation, water chemistry, sulfurization, etc.) on soft-tissue preservation within Holocene-age concretions, which have encapsulated capelin (*Mallotus villosus*). Capelin are small forage fish, which spend most of their life offshore and only enter coastal waters to spawn demersally or on gravely beaches, usually resulting in mass deaths (Nakashima, 2002). We compare and discuss biomarker results from two depositional settings that have produced fossils with contrasting degrees of soft-tissue preservation. The sites are:

Kangerlussuaq, *Greenland*: A marine environment where glacial sediments, recently exposed due to isostatic rebound (Dietrich et al., 2005; Storms et al., 2012), host concretions containing exceptional soft-tissue preservation (Bennike, 1997) (Figure 1a).

Greens Creek, *Ottawa*, *Canada*: Represents the sedimentary remains from the ephemeral brackish-to-freshwater Champlain Sea (Parent & Occhietti, 1988), a marine incursion episode, which harbors concretions mostly containing articulated skeletal remains (Gadd, 1980) (Figure 1b).

The samples from these sites are thermally unaltered carbonate concretions found shallowly buried in sediments, which are similar with respect to the nucleating organic carbon source (i.e., capelin) and relative age (Bennike, 1997; Gadd, 1980). Differences in preservation states may, therefore, be attributable to their contrasting depositional settings, which potentially host varying heterotrophic microbial communities. These fossils thus serve as approximate fossilization experiments under natural conditions to investigate the result of contrasting conditions and underlying soft-tissue preservation mechanisms.

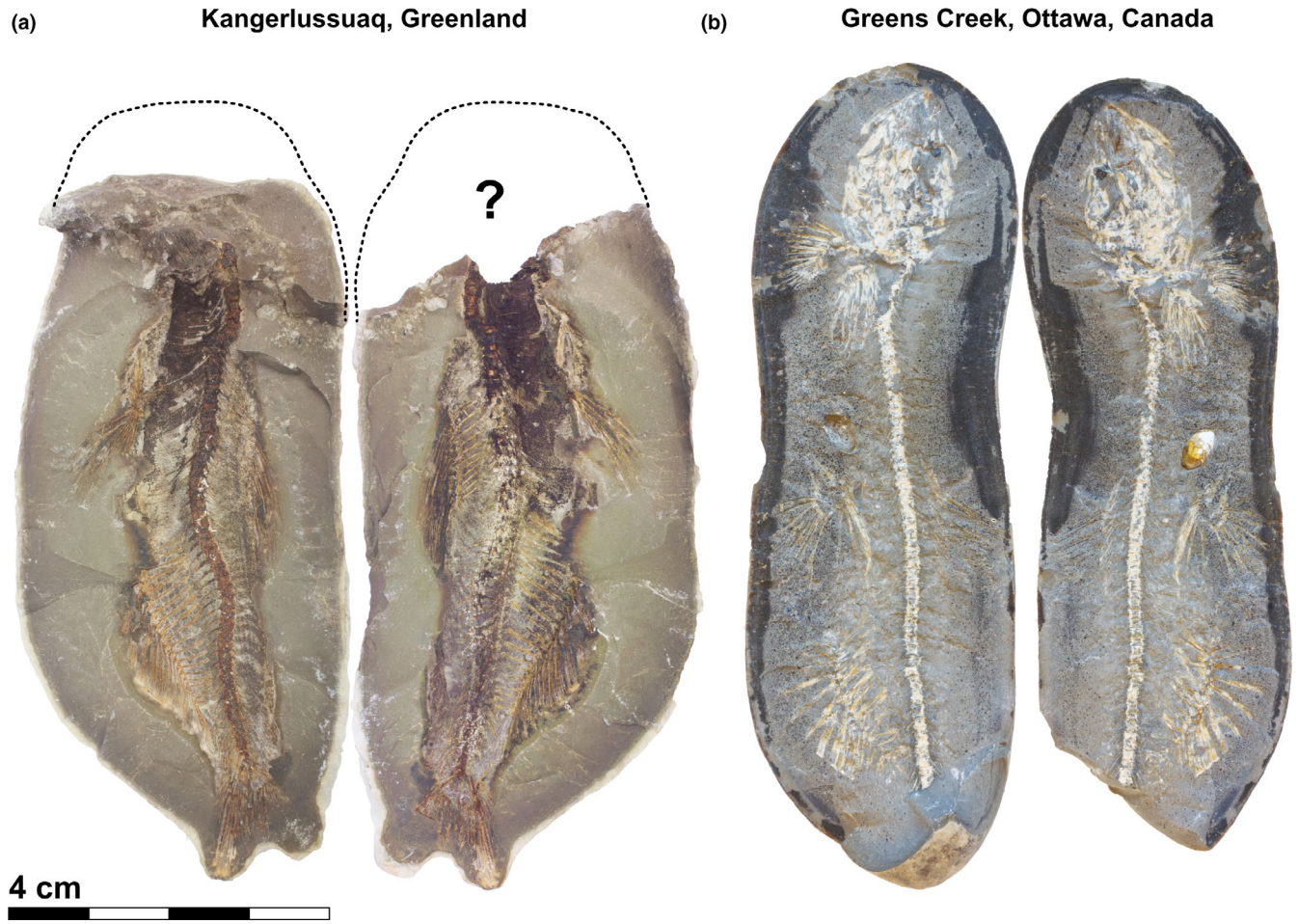

FIGURE 1 Capelin concretions analyzed in this study. The Greenland concretion was collected southwest of the Kangerlussuaq airport (67°00′06.8″N 50°46′19.8″W) by L. Lawaetz while the Canadian concretion was collected from Greens Creek, Ottawa, Ontario (45°27′56.6″N 75°34′34.7″W) by the Geological Survey of Canada (GSC loc. 60327). (a) The Kangerlussuaq concretion does not include a head but otherwise displays exceptional soft-tissue preservation (e.g., organic film in stomach area, skin impressions, color banding), (b) the Ottawa concretion is fully articulated but lacks tissue impressions and stomach contents illustrating a greater degree of decay (each bar is 1 cm)

2 | MATERIALS AND METHODS

2.1 | Site description and sample collection

2.1.1 | Kangerlussuaq, Greenland

The Kangerlussuaq fjord (Danish: Søndre Strømfjord) is a marine environment flanked by highly reworked Archean gneisses inhabited by various species of vascular plants and lichens encompassing its modern catchment (Henkemans et al., 2018). The present-day depth varies between a few meters by the Kangerlussuaq airport (SFJ) near uplifted sediments where concretions have been collected to over 300 m where the mouth of the fjord meets the Davis Strait. During the early Holocene, sea level was approximately 40 m above the present-day land surface at the head of fjord in this paleo tidewater glacier environment. Eventually, it experienced relative sea level decline due to isostatic rebound as the Greenland Ice Sheet (GIS) retreated at the end of the Last Glacial Maximum (LGM) (Dietrich et al., 2005; Storms et al., 2012). This is important because, during deglaciation periods, fjords (and glacial valleys) usually become major sediment sinks due to glacier-induced mass wasting. This results in significant influxes of terrigenous organic matter and nutrients into the water column often inducing eutrophic conditions and bottom water anoxia (Smittenberg et al., 2004). The concretion studied here was collected southwest of the Kangerlussuaq airport at the head of the fjord (c.1960 by Lise Lawaetz) from uplifted sandy glacial sediments where a suite of marine and land vertebrate fossils have been reported by Bennike (1997) (67°00′06.8″N 50°46′19.8″W) (Figure S1).

2.1.2 | Greens Creek, Ottawa, Canada

As the Laurentide ice sheet continued its retreat beyond the Canadian shield from its furthest extent during the LGM, freshwater proglacial Lake Candona was breached by intruding marine waters from the Goldthwait Sea in the isostatically depressed St. Lawrence Valley ~12,400 years ago (Parent & Occhietti, 1988). This event resulted in the ephemeral marine phase recognized as the Champlain Sea, which stood up to 230 m above the present-day Ottawa/Montreal/Burlington region. However, isostatic rebound resulted in the retreat of marine waters ~10,000 years ago followed by the emplacement of modern Lake Champlain (Parent & Occhietti, 1988). Work on depositional facies near Montreal indicate that waters were approximately a mixture of 33% marine and 67% glacial meltwater (Desaulniers & Cherry, 1989a) resulting in brackish-to-freshwater (and possibly estuarine) conditions as previously suggested by the presence of freshwater-tolerant fish fossils at Greens Creek (e.g., capelin, stickleback, sculpin) (McAllister et al., 1981). Palynological analysis of concretion matrices and the discovery of a rare, leopard frog concretion (*Rana pipiens*), indicate the paleo catchment supported shrub tundra communities (Holman et al., 1997). Canadian capelin concretions were generously provided by the Geological Survey of Canada collected from Greens Creek clays derived from the ephemeral Champlain Sea (45°27′56.6″N 75°34′34.7″W) (GSC loc. 60327) (Figure S1).

Samples from both locations have been determined to be Holocene-age through ^{14}C radiocarbon dating techniques (Table 1). Capelin concretions from Kangerlussuaq are about 6000–7000 years old (Brink, 1975) while concretions from Greens Creek have been dated at 10,780 ± 80 years old (Gadd, 1980). Modern capelin, our analytical reference control, were acquired from the Denmark Strait (Icelandic^{+} Capelin Whole Fish).

2.2 | Sample preparation

Concretions were prepared in accordance with similar methods implemented by Melendez, Grice, and Schwark (2013). Approximately 10 mm of each concretion's exposed outer surface was removed by abrading with a Dremel rotary (model 8220-1/28) and diamond cutoff wheel (McMaster-Carr, 1257A33). Approximately ~2 mm thick slices oriented parallel to the fossil nucleus were then taken yielding 4 layers for each specimen (Figure 2). The slices are the fossil layer, matrix 1, matrix 2, and the concretion rim (Figure 2). Biomarker discussions from Greenland and Canada shown here represent analysis from the fossil layer and matrix 1, respectively. These selections were made because of the presence of a carbonaceous film in the Greenland fossil layer while only trace lipids were detected in the Canada fossil layer. Matrix 1 was selected due to its proximity to the nucleus and abundance of detectable compounds. Slices were crushed in a Spex 8510 Shatterbox with a mill and puck cleaned with solvents (i.e., methanol, dichloromethane - DCM, *n*-hexane) and combusted sand (12 h at 850°C) between samples. Recently dead capelin were segmented into different components including the head, tail, internal organs (including heart, stomach, etc.), stomach only, whole fish with internal organs, and whole fish without organs. These were then ground with a tissue homogenizer. All tools (except the Dremel rotary) were solvent cleaned five times with methanol and DCM and combusted at 550°C for 12 h while glassware underwent two dishwasher cycles prior to being combusted at 550°C for 12 h prior to usage. Lipid extractions described below were accompanied by solvent and extraction blanks to determine potential sources of contaminants (if any).

2.3 | Extraction of free lipids (inter-crystalline)

An internal standard (2 μg of 3-methyltricosane) was added to all samples prior to extraction for calculating extraction efficiency. Up to 5 g of the crushed concretion samples were solvent-extracted using a Dionex Accelerated Solvent Extraction (ASE) 350 with DCM-methanol (9:1, v/v) programmed with the following method: cell volume – 34 ml, oven temperature – 100°C, oven heat – 5 min, static time – 15 min, static cycles – 3, flush volume – 130%, purge time – 100 s. Homogenized modern tissue samples (~1 mg each) were solvent-extracted with

TABLE 1 Environment summary, ages, and composition across all samples

	Greenland Summary				Canada			
Environment	Marine				Brackish-fresh[a]			
Estimated age (years)	6000–7000[b]				10,000–11,000[c]			
	Composition							
	Fossil*	Matrix 1	Matrix 2	Rim	Fossil	Matrix 1+	Matrix 2	Rim
TOC (%)	5.50	5.15	5.30	5.10	5.51	5.62	5.54	5.64
Carbonate (%)	57	58	56	57	55	55	56	55

[a]Desaulniers and Cherry (1989a).
[b]Brink (1975).
[c]Gadd (1980).

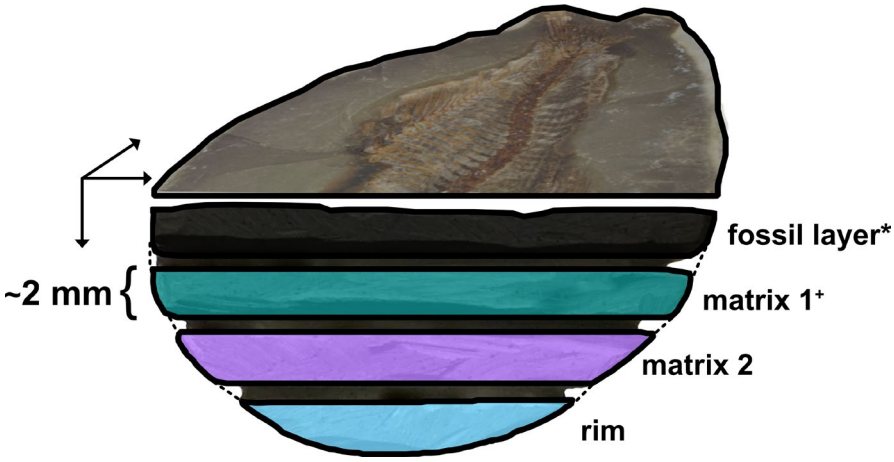

FIGURE 2 Sampling strategy. Approximately 10 mm of each concretion's exposed outer surface was removed via abrasion, ~2 mm thick slices oriented parallel to the fossil nucleus were then taken yielding 4 layers for each specimen (3D exaggeration not to scale). Results shown and discussed here are from the Greenland fossil layer* while results from Canada are from matrix 1+

25 ml DCM-methanol (9:1, v/v) via sonication in 50 ml glass vials in order to prevent probable cross-contamination from organic-rich samples in the ASE. All extracted samples were concentrated to ~1 ml under a steady nitrogen stream on a Zymark Turbovap LV evaporator then transferred into 2 ml vials to evaporate overnight inside an empty fume hood. Dry total lipid extracts (TLEs) were methylated by adding 100 µl of 0.5 N methanolic-HCl (Sigma Aldrich, 07607) to 2 ml vials, which were then tightly capped and heated for 16 h at 60°C in order to convert glycerides and free fatty acids (not to be confused with inter-crystalline free lipids) into fatty acid methyl esters (FAMEs). Derivatized samples were cooled, 100 µl of five-times DCM-cleaned Milli-Q water was then added to quench the reaction and permit extraction from the aqueous phase with 4:1 (v/v) n-hexane-DCM. The (top) organic phase was transferred into 2 ml GC vials with inserts for GC-MS. Samples were concentrated under a gentle nitrogen stream and resuspended in 100 µl *n*-hexane to be analyzed, 50% (50 µl) was taken to be fractionated by column chromatography.

2.4 | Extraction of carbonate-bound lipids (intra-crystalline)

ASE extraction residues from the concretion samples were placed in 500 ml beakers and dissolved by the gradual addition of DCM-washed 2 N hydrochloric acid to release intra-crystalline lipids (O'Reilly et al., 2017). Once dissolution was complete, solutions were diluted with DCM-cleaned water and extracted five times with DCM in a 500 ml separatory funnel by liquid-liquid extraction. As above, the carbonate TLEs were methylated (16 h at 60°C) and split for column chromatography.

2.5 | Copper desulfurization (elemental sulfur removal)

Elemental sulfur (only detected in Greenland TLE chromatograms as a broad hump dominated by *m/z* 64) was removed by incubating the TLEs with 1 g of activated-copper shavings in 4 ml glass vials for 2 h at room temperature. Additional shavings were added if most of the copper darkened due to reacting with sulfur. TLEs were then recovered by rinsing the glass vial five times with DCM.

2.6 | Raney nickel desulfurization (sulfur-bound lipid extraction)

Freshly extracted (i.e., additional subsamples from concretion slices) Greenland TLEs (not Cu-treated as above) underwent Raney

nickel (RN) desulfurization in order to liberate (potentially) sulfur-bound lipids (Sinninghe Damsté et al., 1988). TLEs, initially ASE extracted in 9:1 DCM:MeOH, were gently dried and resuspended in 100 µl distilled absolute ethanol (EtOH > 99.5%) to be transferred into 500 ml conical flasks, each coupled to an Allihn condenser. Five 9-inch glass Pasteur pipette volumes (~10 ml) of RN were added to each conical flask and the reaction was heated to 80°C for 2 h and continuously mixed via a magnetic stir bar. The system was kept anaerobic with a constant nitrogen stream in order to prevent the RN reacting with atmospheric O_2. Desulfurized TLEs were then extracted five times with DCM (liquid-liquid) being careful to avoid the RN becoming dry before deactivation. Subsequently, the non-polar fractions of the desulfurized TLEs were fractionated according to the method below.

2.7 | Column chromatography

TLE splits (free, carbonate-bound, and RN-desulfurized) were fractionated using column chromatography on ~5 g of deactivated silica gel (2% wt H_2O). Three fractions were collected: F1 (saturated hydrocarbons) eluted with 2 dead volumes (DV) of *n*-hexane; F2 (FAMEs and aromatics) eluted with 3 DV of 1:1 (v/v) n-hexane:DCM; F3 (polar lipids) eluted with 2 DV 4:1 (v/v) DCM:MeOH and 1 DV MeOH. F3 samples were concentrated under a gentle nitrogen stream to be derivatized in 25 µl pyridine and 25 µl N,O-Bis(trimethylsilyl)trifluoro-acetamide with trimethylchlorosilane (i.e., BSTFA+TMCS; Sigma Aldrich, 15238) for 1 h at 70°C immediately prior to GC-MS analysis. Raney nickel desulfurized TLEs were separated into two fractions: F1 RN (non-polar lipids) with 4 DV 9:1 *n*-hexane:DCM; F2 RN (polar lipids) with 4 DV 4:1 DCM:MeOH. All fractions, excluding F3 (to be derivatized by BSTFA/pyridine), were concentrated and resuspended in 50 µl *n*-hexane to be analyzed by GC-MS.

2.8 | Gas chromatography-mass spectrometry

Aliquots of the methylated TLEs and subsequent fractions from column separations (F1–F3, F1 RN) were analyzed on an Agilent 6890A gas chromatograph (GC) interfaced with an Agilent 5975C (MS). The GC was equipped with a programmable temperature vaporizer (PTV) inlet (Gerstel) held at 300°C and a J&W DB-5MS fused silica capillary column (60 m × 0.25 mm × 0.25 µm) programmed with the following parameters: 60°C injection and hold for 2 min, ramp at 10°C min^{-1} to 140°C, followed directly by a ramp at 3.5°C min^{-1} to 320°C, and a final isothermal hold at 320°C for 33.6 min.

The MS source was set to 230°C, the quadrupole was set to 150°C, and the MS was operated in electron impact (EI) mode at 70 eV with a scan range between *m/z* 50 to 580. Results were analyzed using Agilent MassHunter Qualitative B.08.00. All reported compounds were identified using a combination of C_8–C_{40} *n*-alkane standards (Sigma Aldrich, 40147-U), $C_{4:0}$–$C_{24:0}$ FAME standards (Sigma Aldrich, 18919-1AMP), steroid standards (e.g., sterol, stanols), mass spectral libraries (NIST17), interpretation of fragmentation patterns, retention times, and comparison to reference literature. Fatty acid identifications were supplemented using a modern capelin tissue reference (Figure S2) and work on fish lipids (Sigurgisladóttir & Pálmadóttir, 1993). Branched-chain fatty acids (BCFA) were identified using fragment ions formed by cleavages adjacent to branch points as determined by Ran-Ressler et al. (2012). Sterol/stanol identifications were supplemented using fragmentation patterns compiled by Prost et al. (2017).

2.9 | Gas chromatography isotope-ratio mass spectrometry

Compound specific carbon isotope ratios of *n*-alkanes (F1) and major fatty acids (F2) were measured on a Trace 1310 gas chromatograph coupled to a MAT253 isotope-ratio mass spectrometer (GC-IRMS) (Thermo Fisher) via a combustion furnace containing copper, nickel, and platinum wires operated at 850°C. The GC was equipped with a PTV injector and a J&W DB-1MS column (60 m × 0.24 mm × 0.25 µm). Measurements were performed in triplicate and are reported in delta notation ($\delta^{13}C$ in per mil, ‰) against Vienna Pee Dee Belemnite. Carbon isotope ratios were corrected for changes in linearity and reproducibility with an *n*-alkane mixture standard (A5, Arndt Schimmelmann, Indiana University) injected after every sample replicate group. The standard deviation for the instrument, based on replicate standard injections, was below 0.4‰. We report data from all concretion slices, albeit, for well-resolved analytes only.

2.10 | Multivariate analysis

Principal component analysis (PCA) is a multivariate statistical method for identifying patterns within large data sets of correlated variables (Hotelling, 1933). PCA has been previously used to identify classes of fossilized tissue (Fabbri et al., 2020; McCoy et al., 2020; Wiemann et al., 2018, 2020) and factors affecting soft-tissue preservation within concretions (McCoy et al., 2015b). We accordingly implement PCA to identify potential relationships between lipid source and preserved soft-tissues. Fatty acids detected in modern capelin along with free and carbonate-bound lipids across all slices (i.e., fossil layer, matrix 1, matrix 2, rim) were defined as variables. Only methylated and diagenetically unaltered fatty acids identified in F2 fractions from column separations were selected for consistency. Therefore, α,ω-dicarboxylic fatty acids and hydroxy fatty acids (which have also been silylated in F3) were not included. The area under each compound (peak) in the total ion chromatogram (TIC), normalized to total organic carbon (g) (see below), was determined using an automated integration script curated with retention times on the Agilent Quantitative Analysis (for GC-MS) B.08.00 software. PCA was executed on GraphPad Prism 9.1.1 software.

2.11 | Bulk composition by loss on ignition

Bulk weight percent total organic carbon and carbonate contents of all concretion slices (fossil, matrix layers, and rim) were estimated by loss on ignition (LOI). 500 mg of each (crushed) concretion slice was weighed on a small ceramic crucible and combusted inside a Barnstead/Thermolyne 30 400 furnace at 550°C for 4 h. Once the samples cooled, the crucibles were re-weighed, and the mass loss was inferred to be the TOC. Samples were re-combusted at 950°C for 2 h, and the subsequent mass loss was inferred to be predominantly from calcium carbonate converted to CaO.

2.12 | Thin sections and targeted electron microprobe analysis

Concretion thin sections, perpendicular to the fossil nucleus (as defined in Section 2.2), were prepared on a Struers Accutom-100 for imaging and elemental analysis at the MIT Electron Microprobe Facility. Thin sections were first photographed on a Zeiss AX10 followed by targeted mineral identification on a JEOL-JXA-8200 Superprobe at a 2-μm aperture.

3 | RESULTS

3.1 | Bulk composition

The total organic carbon of the Greenland and Canada fossil layers was indistinguishable at 5.5%. The carbonate contents were also similar, 57% Greenland and 55% Canada (Table 1). Results for all concretion slices (Greenland & Canada) are found in Table 1.

3.2 | Thin sections and mineral identifications

Both Greenland and Canada thin sections reveal micritic concretion matrices containing sparse detrital inclusions (Figure S3). The Greenland concretion displays irregular radial laminations, which alternate between light and dark bands whereas no laminations were observed in the Canada concretion (Figure S3). The Canada concretion contains detrital quartz, dolomite, and epigenetic manganese dendrites (Seilacher, 2001) while the Greenland concretion contains quartz, apatite, and sulfur-rich amorphous organics (Figures S3 and S4).

3.3 | Saturated hydrocarbons

n-Alkanes (C_{17}–C_{40}) were the predominant saturated hydrocarbons detected from Greenland free lipids (GFL) and carbonate-bound (GCB) fractions along with Canada free lipids (CFL) and carbonate-bound (CCB) fractions (Figure 3). GFL displayed an odd-carbon number preference for long-chain (C_{20}–C_{37}) *n*-alkanes with a maximum (C_{max}) at C_{27} (Figure 3a), GCB did not display a carbon preference and had a C_{max} at C_{29} for long-chain *n*-alkanes (Figure 3a). CFL displayed a C_{max} at C_{18} for short-chain *n*-alkanes (C_{17}–C_{20}), odd-carbon preference, and C_{max} at C_{27} for long-chain *n*-alkanes, and CCB did not display a carbon preference while having a C_{max} at C_{29} (Figure 3b). Calculated pristane/phytane (Pr/Ph) ratios spanning all slices from the fossil layer toward the outer rim were between 0.3–0.4 in GFL and 0.6–1 in CFL samples (Figure 4a). Pristane and phytane could not be detected in the carbonate-bound fractions. Carbon preference index (CPI) (Bray & Evans, 1961) values ranged between 1.94 and 3.6 for GFL, 1–1.1 for GCB, 2.3–3.5 for CFL, and 1.4–1.5 for CCB (Figure 4b). Terrestrial-aquatic ratios for hydrocarbons (TAR_{HC}) (Meyers, 1997) ranged between 7.8–50 for GFL, 100 for GCB, 0.1–0.2 for CFL, and 9.3–18 for CCB (Figure 4c). Total ion chromatograms are available in Figure S5.

3.4 | Fatty acids

Lipid extracts from modern capelin tissues (e.g., tail, with internal organs, stomach only, etc.) yielded the same major fatty acids as those present in muscle (Figure S2), albeit, at varying relative abundances. Fatty acids from Greenland were abundant and diverse in structure. Straight-chain ($C_{14:0}$–$C_{30:0}$), branched-chain (BCFA) ($C_{14:0}$–$C_{17:0}$), monounsaturated (MUFA), and polyunsaturated (PUFA) fatty acids were all detected in GFL (Figure 5a, Table 2) while similar compounds, except for unsaturated fatty acids, were also detected in GCB (Figure 5a, Table 2). GFL long-chain ($C_{20:0}$–$C_{30:0}$) fatty acids displayed an even-carbon preference with a C_{max} at $C_{24:0}$ (Figure 5a), GCB displayed a similar carbon preference with a C_{max} at $C_{20:0}$ (Figure 5a). Fatty acids from CFL exhibited a comparable diversity to GFL. $C_{14:0}$–$C_{30:0}$ straight-chain fatty acids, long-chain fatty acids ($C_{20:0}$–$C_{30:0}$) with a C_{max} at C_{24}, BCFAs ($C_{15:0}$–$C_{17:0}$), and MUFAs were all detected (Figure 5b, Table 2). Straight-chain saturated $C_{14:0}$ - $C_{18:0}$ and $C_{15:0}$ BCFA were the only fatty acids detected in CCB (Figure 5b, Table 2). Both GFL and CFL contained compounds found in modern capelin soft-tissue ($C_{14:0}$, $C_{16:0}$, $C_{18:1\omega9}$, $C_{18:0}$) whereas $C_{18:2\omega6}$, $C_{18:1\omega7}$, $C_{20:1\omega9}$, and $C_{22:1\omega9/11}$ were only detected in GFL (Table 2). $C_{16:1\omega7}$ was the single major monoenoic fatty acid from modern capelin not detected in any concretion sample (Table 2). Terrestrial-aquatic ratios for fatty acids (TAR_{FA}) (Meyers, 1997) were between 0.1–0.3 for GFL, 0–0.4 for CFL, and were 0 for both GCB and CCB (Figure 4d). Notable similarities between Greenland and Canada include: (1) homologous long-chain fatty acid distribution with C_{max} at C_{24}, and (2) detection of 3-Me$C_{16:0}$, 8-Me$C_{16:0}$, 10-Me$C_{16:0}$, 2-Me$C_{16:0}$, 15-Me$C_{16:0}$, and 14-Me$C_{16:0}$ (i.e., branched $C_{17:0}$) BCFAs in GFL, GCB, and CFL. In addition, an abundance of hydroxy fatty acids (OHFA) were detected in Greenland polar fractions, GFL and GCB, including β-OHFA, α-OHFA, and ω-OHFA. β-OHFA dominated between $C_{14:0}$ and $C_{18:0}$ in GFL, while α-OHFA were more prominent between $C_{22:0}$ and

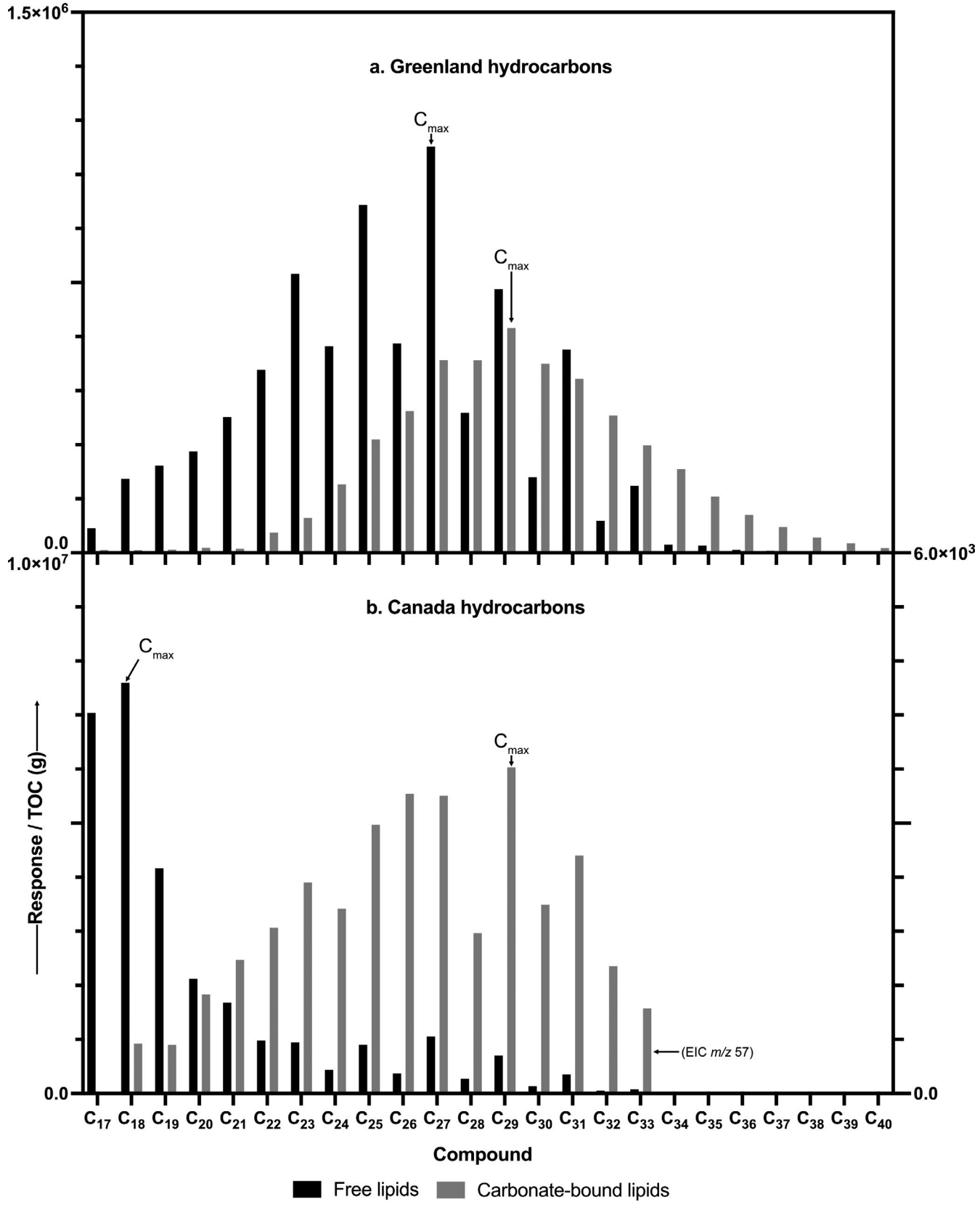

FIGURE 3 Saturated hydrocarbons (F1). (a) Greenland free lipids display an odd-carbon preference for long-chain (C_{20}–C_{37}) *n*-alkanes with a C_{max} at C_{27} while (b) carbonate-bound lipids do not display a carbon preference with a C_{max} at C_{29}. (c) Canada free lipids display an unusual C_{max} at C_{18} while (d) carbonate-bound lipids (right *y*-axis) could only be detected via extracted ion chromatogram (EIC) of *m*/*z* 57 and do not display a carbon preference with a C_{max} at C_{29}

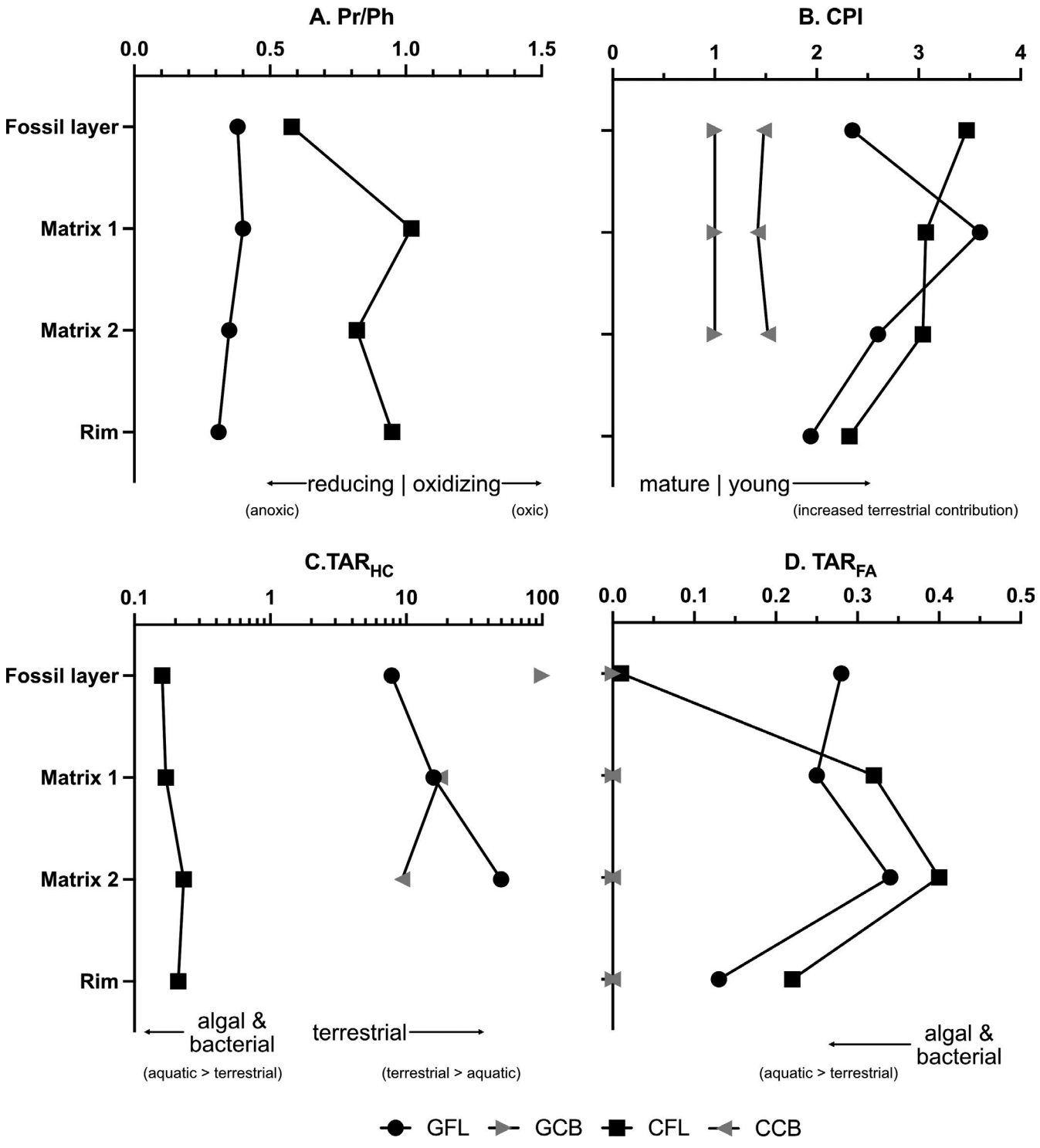

FIGURE 4 Biomarker ratios. (a) Pristane/phytane ratios indicate sustained reducing conditions in Greenland and possibly reducing-to-oxidizing in Canada. (b) Carbon preference index (CPI) generally demonstrates contrasting hydrocarbon maturities have been incorporated into the free lipid and carbonate fractions. (c) Terrigenous/aquatic ratios (TAR_{HC}) for *n*-alkanes demonstrate a higher terrestrial contribution in GFL, GCB, and CCB while CFL shows higher aquatic contributions. (d) Terrigenous/aquatic ratios (TAR_{FA}) for fatty acids show a greater aquatic contribution for all samples

$C_{30:0}$ (Figure S7). ω-OHFA were only detected in $C_{16:0}$ and $C_{22:0}$ carbon lengths in GFL (Figure S7). Lastly, α,ω-dicarboxylic fatty acids (DCFA) were detected in both GCB and CCB (Table 2). Total ion chromatograms are available in Figure S6.

3.5 | Multivariate analysis of fatty acids

Principal component analysis (PCA) performed using fatty acids as variables (excluding hydroxy and dicarboxylic acids) detected

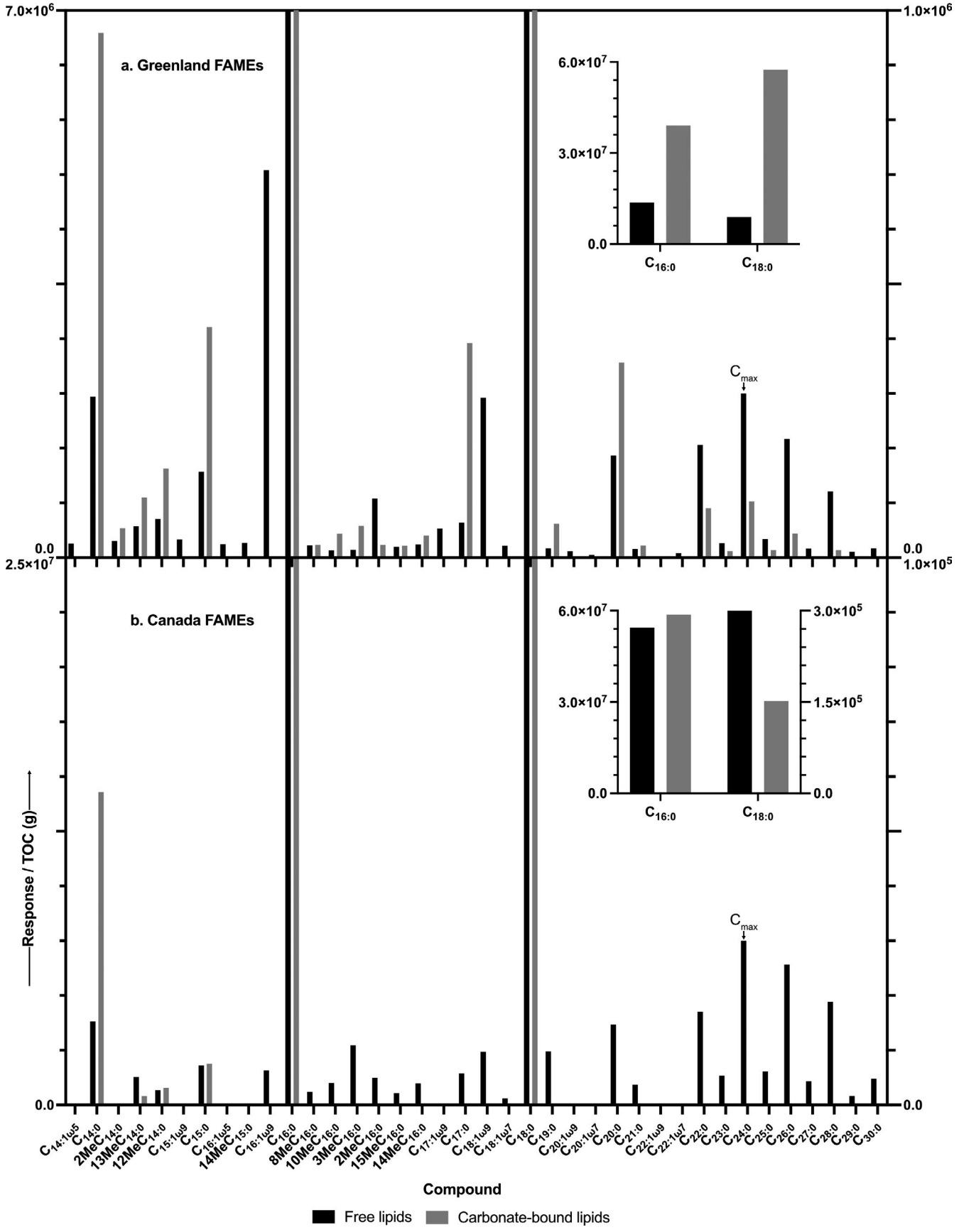

FIGURE 5 Fatty acids (F2). Freely extractable fatty acids from Greenland and Canada were abundant and diverse in structure. (a) Greenland free lipids display an even-carbon preference for long-chain ($C_{20:0}$–$C_{30:0}$) fatty acids with a C_{max} at $C_{24:0}$ while carbonate-bound lipids (right *y*-axis) also display an even-carbon preference but with a C_{max} at $C_{20:0}$. $C_{16:0}$ and $C_{18:0}$ exceeded the *y*-axis window selected here and are, therefore, shown in the small box. (b) Canada free lipids display an even-carbon preference for long-chain ($C_{20:0}$–$C_{30:0}$) fatty acids with a C_{max} at $C_{24:0}$. Carbonate-bond lipids (right *y*-axis) could only be detected via extracted ion chromatogram (EIC) of *m/z* 74 and reveal mostly non-specific short-chain fatty acids ($C_{14:0}$–$C_{18:0}$)

17 PC axes, with the first three explaining more than 15% of variation and 98% of the total variability (Figure 6, Figure S7). PCA biplots for the first three axes simultaneously represent samples and how strongly each variable influences the principal component (Figure 6). Samples are designated as above (i.e., GFL, GCB, CFL, CCB); however, all concretion slices have been included for analysis. The nomenclature used is the following: M1 – modern capelin tissue (female), M2 – modern capelin tissue (male), 0 – fossil layer, 1 – matrix 1, 2 – matrix 2, 3 – rim. For example, GFL0 – Greenland fossil layer free lipids and CCB2 – Canada matrix 2 carbonate-bound lipids. Variance in PC1 is explained by branched $C_{15:0}$ ($13MeC_{14:0}$, $12MeC_{14:0}$), branched $C_{17:0}$ ($3\text{-}MeC_{16:0}$, $8\text{-}MeC_{16:0}$, $10\text{-}MeC_{16:0}$, $2\text{-}MeC_{16:0}$, $15\text{-}MeC_{16:0}$, and $14\text{-}MeC_{16:0}$), and $C_{19:0}$–$C_{30:0}$ straight-chain fatty acids (Figure 6a, Figure S7). Variance in PC2 is explained by unsaturated fatty acids found in modern capelin tissue ($C_{14:0}$, $C_{16:0}$, $C_{16:1\omega9}$, $C_{18:1\omega9}$, $C_{18:1\omega7}$, $C_{20:1\omega9}$, $C_{20:1\omega7}$, $C_{22:1\omega7}$) (Figure 6a, Figure S7). Variance in PC3 is explained by branched $C_{15:0}$ ($2MeC_{14:0}$), branched $C_{16:0}$ ($14MeC_{15:0}$), and unsaturated fatty acids ($C_{14:1\omega5}$, $C_{15:1\omega9}$, $C_{16:1\omega5}$) (Figure 6b, Figure S7).

3.6 | Polar lipids

Following hydrolysis, the lipid extracts from modern capelin tissue samples yielded identical profiles, in this case, cholesterol was the only compound detected (Figure S8). GFL was primarily composed of C_{12}–C_{32} fatty alcohols (*n*-alkanols) with a C_{max} at $C_{22,}$ C_{21}–C_{25} alkan-2-ols, and phytol (Table 2, Figure S7). Major sterols detected in GFL were cholesterol and β-sitosterol along with minor stigmasterol and campesterol. Stanols detected in GFL were coprostanol, epicoprostanol, cholestanol, 5β-stigmastanol, epi-5β-stigmastanol, and 5α-stigmastanol (Table 2, Figure S7). Moreover, C_{30}–C_{32} hopanoids and triterpenoids (i.e., β-amyrin and α-amyrin) were also detected (Table 2, Figure S9). In general, compounds in GCB mirrored GFL except for epicoprostanol, campesterol, and C_{30}–C_{31} hopanoids (Table 2). C_{24}, C_{26}, and C_{28} *n*-alkanols and cholesterol were identified in trace amounts in CFL, no polar lipids were identified in CCB (Table 2).

3.7 | Raney nickel

RN-desulfurized non-polar lipids are dominated by long-chain (C_{21}–C_{40}) *n*-alkanes with a C_{max} at C_{26} and a series of methyl-branched alkanes (Figure S10). Aryl isoprenoids and carotenoids diagnostic of sulfur-oxidizing bacteria were not detected (Figure S10).

3.8 | $\delta^{13}C$ measurements

No corrections were made for the single carbon added by methylation of the fatty acids as experiments with internal standards did not reveal a measurable impact. Saturated hydrocarbon isotope values from GFL, GCB, and CFL varied from −29‰ to −32‰ without a defined structure (Figure 7). Measurements from all samples appear to resemble each other across carbon length, site (Greenland vs. Canada), and source (free vs. carbonate-bound) (Figure 7). Short-chain ($C_{14:0}$–$C_{18:0}$) and monoenoic fatty acid carbon isotope values from GFL, GCB, and CFL varied between −24‰ to −30‰, in contrast, long-chain ($C_{19:0}$–$C_{30:0}$) fatty acid measurements for GFL and GCB varied between −28‰ to −32‰ (Figure 8).

4 | DISCUSSION

4.1 | Results overview

Two concretions from glacial environments (marine vs. brackish-to-freshwater), comparable age, and similar organic carbon sources (capelin) have produced highly contrasting fossil end-members (soft-tissue present vs. no soft-tissue) (Figure 1). Due to their relatively young age and shallow burial depths, thermal diagenesis is inferred to have been negligible. Thus, these concretions serve as approximate fossilization experiments found under natural conditions. Lipids extracted from the concretion free fraction (inter-crystalline) appear to be derived from more diverse (and possibly geologically recent) organic sources (e.g., vascular plants, algae, sulfate-reducing bacteria) (Table 2) (Ackman et al., 1968; Bianchi & Canuel, 2011; Drenzek et al., 2007; O'Reilly et al., 2017; Rielley et al., 1991; Volkman et al., 1980). In contrast, carbonate-bound lipids (intra-crystalline) have a relatively lower diversity and exhibit more diagenetically altered byproducts (e.g., dicarboxylic acids, stanols, loss of carbon preference), which may coincide with carbonate precipitation/concretion growth (Table 2) (Bray & Evans, 1961; Volkman, 2006). Results from all concretion slices are reported in Figures S11-S15.

4.2 | Greenland lipid sources & paleoenvironmental conditions

4.2.1 | Vascular plant lipids

GFL long-chain (C_{20}–C_{37}) *n*-alkanes containing an odd-carbon preference, and C_{max} at C_{27} represent a predominant input from land plant leaf waxes (Figure 3a) (Eglinton & Hamilton, 1967). Long-chain ($C_{20:0}$–$C_{30:0}$) even-carbon preference fatty acids (Figure 5a) and

TABLE 2 Compound identification, abbreviations, and sample detection

Compound	Abbreviation(s)	Modern	Greenland		Canada	
			Free	Carbonate	Free	Carbonate
n-Alkyl compounds						
n-Alkanes	C_{16} … C_{38}	−	+	+	+	+
Branched-chain alkanes	brC_{17} … brC_{20}	−	+	−	+	−
n-Alkanols	$C_{12\text{-}1}$ … $C_{32\text{-}1}$	−	+	+	+	−
Alkan-2-ols	$C_{21\text{-}2}$ … $C_{25\text{-}2}$	−	+	+	−	−
Methyl *n*-ketones	C_{19} … C_{33}	−	−	−	+	−
Fatty acids						
Straight-chain saturated fatty acids (<20 carbons)	$C_{14:0}$ … $C_{19:0}$	+	+	+	+	+
Long-straight-chain saturated fatty acids	$C_{20:0}$ … $C_{30:0}$	−	+	+	+	−
12-Methyl tridecanoic acid ($C_{14:0}$ iso)	$12MeC_{13:0}$	−	+	+	−	−
Tetradec-9-enoic acid	$C_{14:1\omega5}$	−	+	−	−	−
2-Methyl tetradecanoic acid	$2MeC_{14:0}$	−	+	+	−	−
13-Methyl tetradecanoic acid ($C_{15:0}$ iso)	$13MeC_{14:0}$	−	+	+	+	+
12-Methyl tetradecanoic acid ($C_{15:0}$ anteiso)	$12MeC_{14:0}$	−	+	+	+	+
Pentadec-6-enoic acid	$C_{15:1\omega9}$	−	+	−	−	−
Hexadec-11-enoic acid	$C_{16:1\omega5}$	−	+	−	−	−
14-Methyl pentadecanoic acid ($C_{16:0}$ iso)	$14MeC_{15:0}$	−	+	−	−	−
Hexadec-9-enoic acid	$C_{16:1\omega7}$	+	−	−	−	−
Hexadec-7-enoic acid	$C_{16:1\omega9}$	−	+	−	+	−
3-Methyl hexadecanoic acid	$3\text{-}MeC_{16:0}$	−	+	+	+	−
8-Methyl hexadecanoic acid	$8\text{-}MeC_{16:0}$	−	+	+	+	−
10-Methyl hexadecanoic acid	$10\text{-}MeC_{16:0}$	−	+	+	+	−
2-Methyl hexadecanoic acid	$2\text{-}MeC_{16:0}$	−	+	+	+	−
15-Methyl hexadecanoic acid ($C_{17:0}$ iso)	$15\text{-}MeC_{16:0}$	−	+	+	+	−
14-Methyl hexadecanoic acid ($C_{17:0}$ anteiso)	$14\text{-}MeC_{16:0}$	−	+	+	+	−
Heptadec-10-enoic acid	$C_{17:1\omega9}$	−	+	−	−	−
Octadeca-9,12-dienoic acid	$C_{18:2\omega6}$	+	+	−	−	−
Octadec-9-enoic acid	$C_{18:1\omega9}$	+	+	−	+	−
Octadec-11-enoic acid	$C_{18:1\omega7}$	+	+	−	+	−
icos-11-enoic acid	$C_{20:1\omega9}$	+	+	−	−	−
docos-11-enoic acid	$C_{22:1\omega11}$	+	+	−	−	−
docos-13-enoic acid	$C_{22:1\omega9}$	+	+	−	−	−
α-Hydroxy fatty acids	$\alpha C_{22:0}$ … $\alpha C_{30:0}$	−	+	+	−	−
β-Hydroxy fatty acids	$\beta C_{14:0}$ … $\beta C_{18:0}$	−	+	+	−	−
$C_{15:0}$ methyl-branched β-hydroxy fatty acids	$a\beta C_{15:0}$, $i\beta C_{15:0}$	−	+	+	−	−
ω-Hydroxy fatty acids	$\omega C_{16:0}$, $\omega C_{22:0}$	−	+	+	−	−
Dicarboxylic fatty acids	α,ω-fa	−	−	+	−	+

TABLE 2 (Continued)

Compound	Abbreviation(s)	Modern	Greenland		Canada	
			Free	Carbonate	Free	Carbonate
Steroids						
5β-Cholestan-3β-ol (coprostanol)	$C_{27}^{5\beta,3\beta}$	–	+	+	–	–
5β-Cholestan-3α-ol (epicoprostanol)	$C_{27}^{5\beta,3\alpha}$	–	+	–	–	–
Cholest-5-en-3β-ol (cholesterol)	$C_{27}\triangle^{5}$	+	+	+	+	–
5α-Cholestan-3β-ol (cholestanol)	$C_{27}^{5\alpha,3\beta}$	–	+	+	–	–
24-Methyl-cholest-5-en-3β-ol (campesterol)	$C_{28}\triangle^{5,22}$	–	+	–	–	–
24β-Ethyl-5β-cholestan-3β-ol (5β-stigmastanol)	$C_{29}^{24\beta,5\beta,3\beta}$	–	+	+	–	–
24β-Ethyl-5β-cholestan-3α-ol (epi-5β-stigmastanol)	$C_{29}^{24\beta,5\beta,3\alpha}$	–	+	+	–	–
24-Ethyl-cholest-5,22-dien-3β-ol (stigmasterol)	$C_{29}\triangle^{5,22}$	–	+	+	–	–
24-Ethyl-cholest-5-en-3β-ol (β-sitosterol)	$C_{29}\triangle^{5}$	–	+	+	–	–
24α-Ethyl-5α-cholestan-3β-ol (5α-stigmastanol)	$C_{29}^{24\beta,5\alpha,3\beta}$	–	+	+	–	–
Hopanoids						
17β,21β(H)-hopan-30-ol	$\beta\beta C_{30}$	–	+	–	+	–
17β,21β(H)-hopan-31-ol	$\beta\beta C_{31}$	–	+	–	+	–
17β,21β(H)-Bishomohopan-32-ol	$\beta\beta C_{32}$	–	+	+	–	–
Terpenoids						
3α-hydroxy-5β-cholanic acid (lithocholic acid)	LCA	–	–	+	–	–
β-Amyrin	β-am	–	+	+	–	–
α-Amyrin	α-am	–	+	+	–	–
11-oxo-α-amyrin	oxo-α-am	–	+	–	–	–
Miscellaneous						
Norpristane	npr	–	–	–	+	–
Pristane	pr	–	+	–	+	–
Phytane	ph	–	+	–	+	–
Phytol	phy	–	+	+	–	–
Pyrene	py	–	+	–	+	–
Retene	re	–	–	–	+	–

triterpenoid alcohols (i.e., amyrin) in both GFL and GCB (Table 2) further suggest input from vascular plants (Bianchi & Canuel, 2011; Řezanka, 1989; Rielley et al., 1991). Accordingly, $\delta^{13}C$ values between −29‰ to −32‰ for *n*-alkanes (C_{20}–C_{37}) (Figure 7) and −28‰ to −32‰ for fatty acids ($C_{19:0}$–$C_{30:0}$) (Figure 8) typical for C3 plants appear to confirm this interpretation (Drenzek et al., 2007; Volkman, 2006). Interestingly, the lack of carbon preference in GCB *n*-alkanes (Figure 3a) and C_{max} at C_{29} may indicate contribution from a catchment-derived mature hydrocarbon (Bray & Evans, 1961). CPI values (Figure 4b) further demonstrate contrasting terrestrial sources have been incorporated into the free lipid (GFL > 1) and carbonate fractions (GCB = 1) (Bray & Evans, 1961). High TAR_{HC} ratios at Greenland indicate greater terrestrial (i.e., vascular plants) hydrocarbon contribution versus aquatic (i.e., algal & bacterial) (Figure 4c).

4.2.2 | Algal lipids

C_{28}–C_{29} phytosterols (campesterol, stigmasterol, and sitosterol), branched $C_{16:0}$ ($14MeC_{15:0}$), monounsaturated fatty acids ($C_{14:1\omega5}$, $C_{15:1\omega9}$, $C_{16:1\omega5}$, $C_{17:1\omega9}$), and fatty alcohols (*n*-alkanols) suggest contribution and enhanced primary productivity by microalgae (Ackman et al., 1968; Volkman, 2006; Volkman et al., 1980, 1998). TAR_{FA} ratios indicate greater aquatic contributions of fatty acids (Figure 4d) (Meyers, 1997).

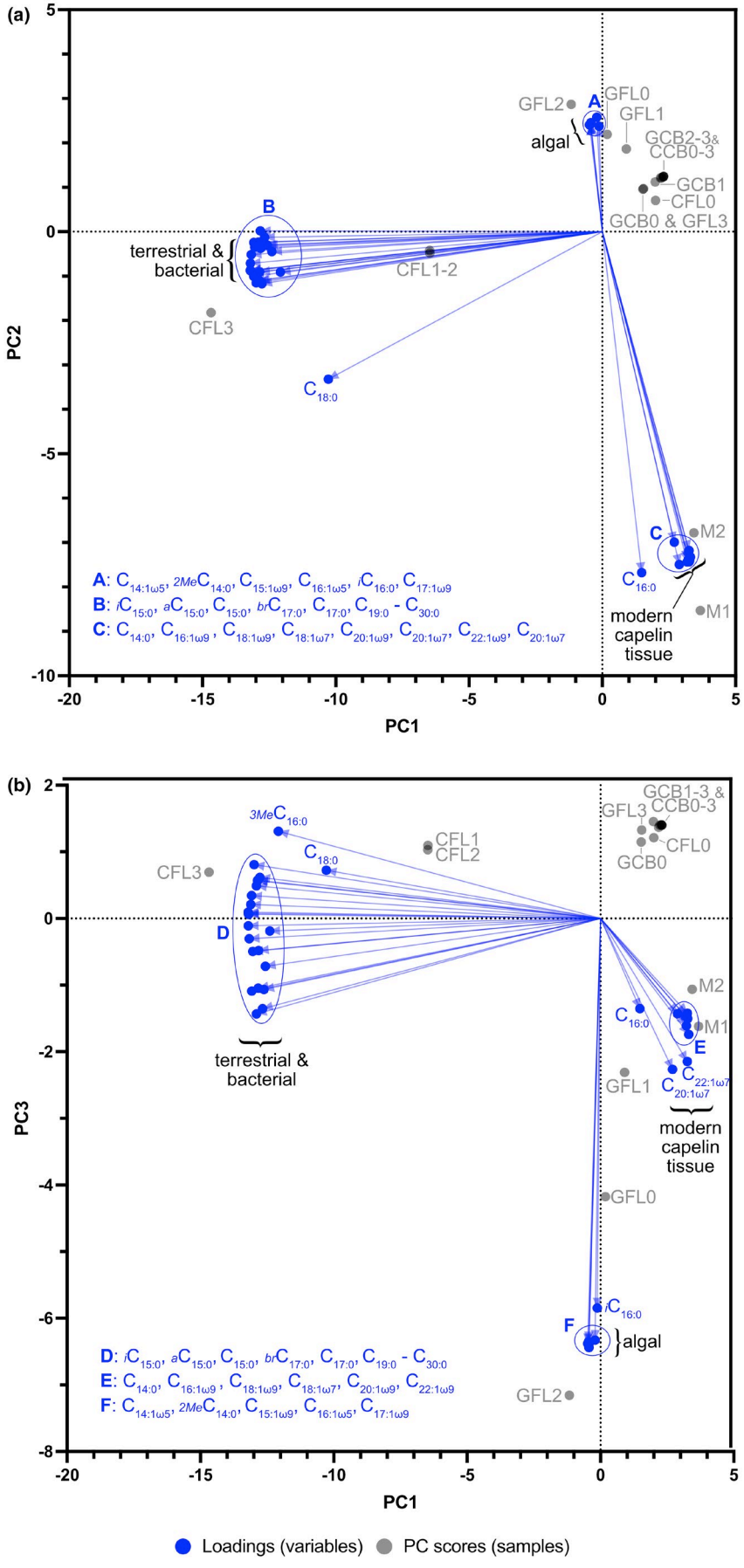

FIGURE 6 Principal component analysis. Fatty acids found across all samples and in modern capelin were designated as variables and their values are represented by the integrated area (response/TOC (g)) in the F2 total ion chromatogram (TIC). (a) PC1 vs PC2. (b) PC1 vs PC3. Blue circles do not indicate statistical significance; however, they are used to identify compounds, which are too tightly grouped to discretely label. (a) CFL samples are most influenced by bacterial and environmental lipids in PC1, (b) GFL samples are most influenced by algal lipids in PC2, (c) GFL samples are influenced by a mixture of algal lipids and capelin soft-tissue in PC3, and CFL0 groups with carbonate fractions

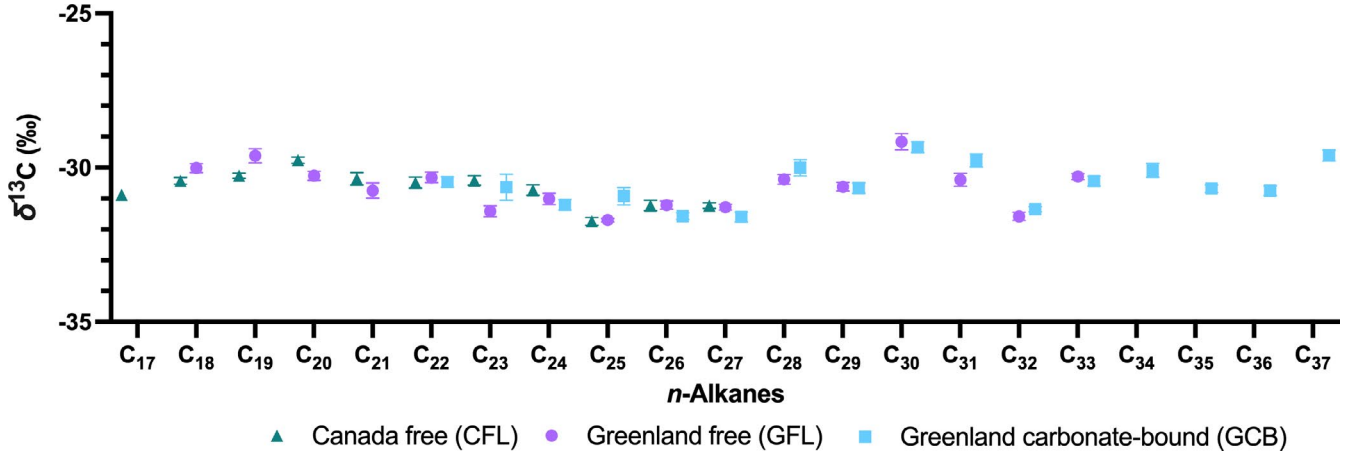

FIGURE 7 Saturated hydrocarbon fraction $\delta^{13}C$ data (F1). Isotope measurements from both Kangerlussuaq and Ottawa varied from −29‰ to −32‰ without defined structure. Canada free $n = 6$, Greenland free $n = 9$, Greenland carbonate-bound $n = 6$

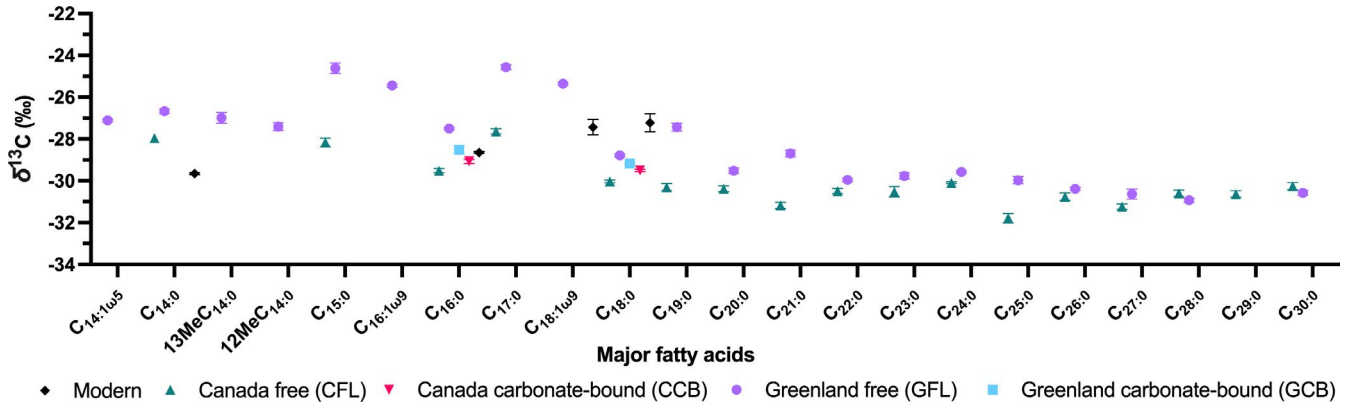

FIGURE 8 Major fatty acid $\delta^{13}C$ data. Short-chain ($C_{14:0}$–$C_{18:0}$) isotope measurements varied from −24‰ to −30‰. Long-chain ($C_{19:0}$–$C_{30:0}$) measurements spanned a narrower range −28‰ to −32‰. Modern $n = 3$, Canada free $n = 6$, Canada carbonate-bound = 6, Greenland free $n = 9$, Greenland carbonate-bound $n = 6$

4.2.3 | Bacterial lipids

Short-chain fatty acids ($C_{14:0}$–$C_{19:0}$) detected in both GFL and GCB (along with the presence of elemental sulfur in chromatograms *m/z* 64) suggest a close association with sulfate-reducing bacteria (SRB). Branched $C_{17:0}$ fatty acids (Table 2), namely, 10-Me$C_{16:0}$, are particularly diagnostic for Deltaproteobacteria (Dowling et al., 1986; Taylor & Parkes, 1983) and have been identified in cultures of *Desulfobacter* and in areas harboring persistent SRB communities (Elvert et al., 2003; Hinrichs et al., 2000).

4.2.4 | Paleoenvironment

Altogether, lipid biomarker results are comparable to contemporary eutrophic fjords (e.g., Smittenberg et al., 2004). Bottom waters at Kangerlussaq were most likely reducing (Figure 4a, Pr/Ph: 0.3–0.4) and sulfidic maintained by enhanced biological sulfate reduction in response to glacier-induced mass wasting (and organic matter input). The lack of detectable aromatic carotenoids, however, does not indicate sulfidic conditions in the photic zone (Figure S10) (Melendez, Grice, Trinajstic, et al., 2013). PCA results indicate variance in GFL samples (e.g., fossil layer to rim) is best explained by a mixture of algal lipids and capelin soft-tissue (Figure 6b).

4.3 | Canada lipid sources & paleoenvironmental conditions

4.3.1 | Vascular plant lipids

Like Greenland, CFL long-chain (C_{20}–C_{37}) *n*-alkanes containing an odd-carbon preference and C_{max} at C_{27} likely represent input from land plants (Figure 3b) (Eglinton & Hamilton, 1967). CCB trace hydrocarbons (like GCB) with an apparent lack of carbon preference and C_{max} at C_{29} indicates a mature hydrocarbon input from the surrounding catchment (Figure 3b; Figure 3a) (Bray & Evans, 1961). CPI values for CFL and CCB mirror those of GFL and GCB suggesting terrestrial

sources with contrasting maturities have been incorporated into free and carbonate-bound fractions. Homologous long-chain ($C_{20:0}$ - $C_{30:0}$) even-carbon-number preference fatty acids with C_{max} at $C_{24:0}$ (Figure 5b) and $\delta^{13}C$ values consistent with C3 plants support input from terrestrial vascular plants (Figure 8) (Bianchi & Canuel, 2011; Řezanka, 1989; Rielley et al., 1991). Still, we note that others have attributed this fatty acid pattern to a microbial source (Řezanka et al., 1990; Summons et al., 2013).

4.3.2 | Algal lipids

TAR_{HC} and TAR_{FA} ratios (<1) both indicate greater aquatic contributions (algal & bacterial) over terrestrial (Meyers, 1997). However, CFL short-chain *n*-alkanes (C_{17}–C_{20}) exhibit an unusual C_{max} at C_{18} possibly attributable to sulfate-reducing bacteria (discussed below). C_{17} to C_{20} $\delta^{13}C$ values between −29‰ to −32‰ could represent a likely mixed bacterial-algal source (McKirdy et al., 2010; Volkman, 2006). Phytosterols and unsaturated fatty acids diagnostic of aquatic inputs are absent in both CFL and CCB (Table 2). Only C_{24}, C_{26}, and C_{28} *n*-alkanols were identified in CFL (Table 2) (Volkman et al., 1998).

4.3.3 | Bacterial lipids

CFL hydrocarbons display an unusual C_{max} at $C_{18,}$ which have previously been attributed to bacterial origins in marine sediments (Aloulou et al., 2010; Grimalt & Albaigés, 1987; Nishimura & Baker, 1986). Work by Davis (1968) demonstrated that cultures of the sulfate-reducing bacterium *Desulfivibrio desulfuricans* produce comparable *n*-alkane profiles; however, unusual *n*-alkane distributions have also been detected from other marine bacteria and algae (Han & Calvin, 1969). In this instance, the co-occurrence of branched $C_{17:0}$ BCFA in CFL and CCB suggests a likely association with sulfate-reducing bacteria like in Greenland (Figure 5, Table 2) (e.gDowling et al., 1986; Taylor & Parkes, 1983).

4.3.4 | Paleoenvironment

Given the dearth of lipid biomarker information, we are unable to clearly establish environmental conditions at the time of concretion formation. Pristane/phytane values indicate possibly reducing bottom waters (anoxic) (Figure 4a), which are required to prevent scavenging and permit the preservation of fully articulated fish remains (Allison, 1988a; McAllister et al., 1981). Hydrogeological studies of clays, minerals, and porewaters emplaced during the Champlain Sea suggest the widespread occurrence of sulfate reduction as pyrite and HCO_3^- concentrations in saturation have been recorded (Desaulniers & Cherry, 1989b). However, SRB activity would have most likely been attenuated by low SO_4^{2-} concentrations, which are predicted to have approached zero due to dilution from seasonal glacial discharge (Cronin et al., 2008). Lipid biomarker results appear more consistent with low productivity (pelagic) waters or perhaps generally reflect the decreased preservation potential at Greens Creek. PCA results indicate variance in CFL samples is best explained by bacterial and environmental lipids (Figure 6).

4.4 | Hypotheses for mechanisms resulting in soft-tissue preservation

The diverse assemblage of lipids identified in this study, morphological features, and the detection of nearly all lipids found in the reference capelin (except for $C_{16:1\omega7}$) demonstrate that the Greenland concretion is an example of exceptional soft-tissue preservation (Figures 1, 5, and 6). This contrasts with the Canada concretion, which is mostly devoid of soft tissue and is overrepresented by environmental and bacterial signals (Figures 1, 5, and 6). At Kangerlussuaq, Greenland, sulfate-reducing bacteria (SRB) appear to be the principal mediators of concretion formation under a eutrophic regime induced by glacial mass wasting. Aquatic and terrestrial lipids are characterized by long-chain *n*-alkanes, monounsaturated fatty acids, polyunsaturated fatty acids, long-chain fatty acids, hydroxy fatty acids, *n*-alkanols, phytosterols, and triterpenoids (Table 2). At Greens Creek, although SRB lipids have been identified, it remains unclear whether additional microbial communities were involved in concretion formation and how productive waters may have been. Using the presented data, we propose preservation biases within concretions can be determined by evaluating two alternate hypotheses, which weigh the importance of specific bacterial communities (i.e., sulfate-reducing bacteria) versus depositional parameters on exceptional preservation:

I Enhanced preservation occurs due to SRB activity resulting in euxinic conditions, which result in H_2S-lipid interactions that impart labile compounds resistance to decay (Adam et al., 2000; Hebting, 2006; Melendez, Grice, & Schwark, 2013; Melendez, Grice, Trinajstic, et al., 2013).

II Enhanced preservation occurs due to depositional parameters (e.g., primary productivity, organic matter input, sediment porosity, diffusion, porewater velocity, and solute concentrations), which determine favorable alkalinity gradients and mediate the rate of carbonate precipitation (Berner, 1968a, 1968b; Berner et al., 1970). That is, exceptional soft-tissue preservation within concretions may fundamentally represent a race between carbonate precipitation and decay (Sagemann et al., 1999).

4.5 | Controls on capelin soft-tissue preservation at Greenland and Canada

Taphonomic experiments have suggested that microbial communities involved in decay may paradoxically be responsible for increased preservation (e.gAllison, 1988b; Briggs, 2003; Briggs & Kear, 1993;

Briggs & McMahon, 2016; Butler et al., 2015; Gäb et al., 2020; Iniesto et al., 2013; Sagemann et al., 1999). Early microbial colonization and production of biofilms may enhance the preservation of morphological features while decay can stimulate mineral replacement (e.g., pyritization, phosphatization) and/or the encapsulation of soft tissues (e.g., concretion formation). Furthermore, H_2S-rich (euxinic) environments sustained by SRBs have been shown to mediate the preservation of organic compounds via macromolecular incorporation and reduction (Adam et al., 2000; Hebting, 2006; Melendez, Grice, Trinajstic, et al., 2013).

Biomarker results indicate SRB may have been responsible for concretions at Greenland and Canada as branched-chain fatty acids ($brC_{17:0}$) (Figure 5) and an unusual *n*-alkane C_{max} (C_{18}) (Figure 3b) were detected. However, two key differences between locations are the detection of endogenous capelin tissue and significant algal lipids in Greenland (Figure 6, Table 2). This is important because biomarker results from Greenland illustrate a highly productive water column fed by glacier-induced mass wasting resulting in massive organic matter input into fjord bottom waters. In particular, bacterial sulfate reduction has been shown to be directly proportional to organic matter input, not sulfate availability (Edenborn et al., 1987; Jørgensen et al., 1982). A key implication is that bottom waters at Kangerlussuaq fjord likely sustained a considerable bicarbonate (HCO_3^-) reservoir from enhanced SRB activity (Berner, 1968b). Then, as capelin mortality events occurred due to spawning, depositional conditions were conducive toward rapid carbonate encapsulation (Berner, 1968a). In contrast, biomarker results from Canada appear more consistent with relatively unproductive waters and negligible organic matter input from the environment. Therefore, capelin decay may have directly contributed toward concretionary growth in lieu of an environmental bicarbonate reservoir (Berner, 1968a).

Although biomarker results indicate the presence of SRB at both sites, we are unable to ascribe preservation differences observed between sites to Hypothesis I. First, the presence of SRB shows no relationship to capelin soft-tissue preservation (Figure 6). CFL samples are most influenced by bacterial and environmental lipids in PC1 (Figure 6a), GFL samples are most influenced by algal lipids in PC2 (Figure 6a), and GFL samples are influenced by a mixture of algal lipids and capelin soft-tissue in PC3 (Figure 6b). Second, reduction and sulfurization of lipids do not appear to be key abiotic processes contributing to increased preservation at Greenland due to readily extractable and labile lipids in both free and carbonate-bound fractions (e.g., MUFAs, PUFAs, sterols, etc.). In particular, because sulfate reduction in marine environments is regulated by organic matter input, SRB activity at Kangerlussuaq may have been key toward sustaining particular porewater chemistries rather than enabling indirect abiotic preservation mechanisms. Hypothesis II, therefore, represents a viable proposition, which emphasizes the depositional context (i.e., primary productivity, organic matter input, etc.) on the rate of concretion formation. In support of this, taphonomic experiments and statistical analysis of environmental parameters (i.e., host lithology, mineral composition, water chemistry, etc.) have emphasized the role of authigenic precipitation on exceptional preservation (Allison, 1988b; Briggs, 2003; McCoy et al., 2015a, 2015b; Sagemann et al., 1999). As microbial decay induces carbonate precipitation within shallow sediments, cementing pore spaces impede electron acceptor flow (e.g., SO_4^{2-}) into the decay foci resulting in attenuated microbial respiration (McCoy et al., 2015a, 2015b). Thus, it is important to understand how environmental parameters such as organic matter delivery, primary productivity, microbial respiration rates, sedimentation rate, and lithology could conceivably affect the post-depositional setting and influence concretion formation.

4.6 | Concretion formation at Greenland and Canada

Studies on concretion formation have generally noted that if porewaters are adequately supersaturated (i.e., SI > 0.8, Kempe & Kazmierczak, 1994), unremarkable bodies can act as simple nucleators (e.g., detritus, shells) for carbonate precipitation (Coleman & Raiswell, 1995; Pye et al., 1990; Raiswell, 1976). Conversely, in other environments, decaying organism may become the primary source of alkalinity driving precipitation (Coleman, 1993; Coleman & Raiswell, 1995; Raiswell, 1976). Early work by Berner (1968a) hypothesized that in supersaturated porewaters (i.e., 10 ppm $CaCO_3$), the rate of concretion growth may be modeled as a function of porewater velocity. That is, carbonate precipitation rates in stagnant post-depositional settings are diffusion-limited and slow, meanwhile, precipitation rates in non-diffusion-limited sediments are much faster. Work by Desaulniers and Cherry (1989a) has shown that sediments in the Ottawa Valley immediately adjacent to Greens Creek are composed of marine clays with measured porewater velocities (i.e., 2 m/year) on-par with (modeled) stagnant, diffusion-limited, concretion formation (Berner, 1968a). On the other hand, while velocities are not available from Kangerlussuaq, measurements of analogous glacial deposits from Norwegian fjords estimate an excess of 100 m/year (Soldal et al., 1994; Soldal & Rye, 1995). These observations suggest organic matter input, decay rates, and post-depositional properties are parameters, which greatly influence the rate of concretion formation.

Modeled precipitations rates outlined in Berner (1968a) predict the Kangerlussuaq concretion (concretion radius = 1.5 cm, porewater velocity = 100 m/yr) could have formed within ~400 years and Greens Creek (concretion radius = 1.4 cm, porewater velocity = 2 m/yr) within ~1000 years. Accordingly, preliminary radiocarbon measurements across concretion transects reflect concentric growth patterns, out-to-in, which occurred within 450-years for Greenland and 1100-years for Canada (Mojarro et al., 2021). However, further investigation is required to confirm age trends and exclude possible mixing signals of old and young carbon that might introduce artifacts. Still, key implications are that: (1) low-permeability clays at Greens Creek may have impeded porewater circulation leading to decreased precipitation rates and persistent decay by SRB (and subsequently by other microbes as SO_4^{2-} became scarce) resulting in the complete remineralization of capelin

tissues; (2) high-permeability sandy sediments supplemented by likely supersaturated carbonate porewaters (as indicated by organic matter input) at Kangerlussuaq facilitated rapid concretion formation. Given lipid analysis, modeling work, and known depositional parameters, we conclude preservation differences observed between Canada and Greenland represent varying rates of concretion formation (i.e., Hypothesis II).

5 | CONCLUSIONS

Fish are commonly found in concretions, but the very recent occurrence of the same taxon (capelin) in different depositional environments has offered a unique opportunity to explore processes resulting in soft-tissue preservation. Here we have presented a comparative biomarker analysis of Holocene-age concretions from two environments that have produced highly contrasting fossils. (1) Kangerlussuaq, Greenland: a marine environment with recently exposed sediments due to isostatic rebound, and (2) Greens Creek, Ottawa, Canada: a paleo brackish-to-freshwater marine episode that resulted from the retreat of the Laurentide ice sheet. Given lipid biomarker evidence, we have determined that eutrophic conditions mediated enhanced rates of sedimentary sulfate reduction resulting in porewater carbonate supersaturation at Kangerlussuaq. Porous sandy sediments then permitted rapid porewater velocities (e.g., non-diffusion-limited) resulting in a subsequent increase of carbonate precipitation rates accounting for soft-tissue preservation. We propose that exceptional preservation within concretions possibly occurs via the following steps and, in its simplest iteration, represents a race between precipitation and decay: (1) organic matter input feeds heterotrophic microbial communities sustaining large carbonate reservoirs, (2) high porewater velocities replenish ions (e.g., HCO_3^-, Fe^{2+}, Ca^{2+}, etc.) spent at sites of active precipitation, and 3) decay decreases (and ultimately ceases) in response to a cementing-pore space. It remains unknown whether Greens Creek concretions were the sole byproducts of SRB or a microbial consortium of sulfate-reducers, iron-reducers, or methanogens (for instance) because of the predicted seasonal limitation of SO_4^{2-}. If so, microbes using lower-efficiency redox couples did not necessarily yield an increased preservation potential at Greens Creek. Lastly, while the role of H_2S was not explicitly involved with enhanced biomarker preservation at Kangerlussuaq, Raney nickel desulfurization experiments confirmed the presence of a recalcitrant sulfurized macromolecular fraction, which have been observed to persist over geological timescales.

ACKNOWLEDGMENTS

This work was supported by the MIT Dean of Science Fellowship. Laboratory work at MIT was supported by the Simons Foundation, Collaboration on the Origins of Life (SCOL) through an award (290361FY18) to RES. We would like to thank Michelle Coyne at the Geological Survey of Canada, Professor Derek Briggs, Ben Uveges, and Lise Lawaetz.

CONFLICT OF INTEREST

No competing financial interests exist.

DATA AVAILABILITY STATEMENT

The data that support the findings of this study are available from the corresponding author upon reasonable request.

ORCID

Angel Mojarro https://orcid.org/0000-0003-4547-4747
Xingqian Cui https://orcid.org/0000-0001-6705-7595
Xiaowen Zhang https://orcid.org/0000-0001-8768-1459
Jakob Vinther https://orcid.org/0000-0002-3584-9616
Roger E. Summons https://orcid.org/0000-0002-7144-8537

REFERENCES

Ackman, R. G., Tocher, C. S., & McLachlan, J. (1968). Marine phytoplankter fatty acids. *Journal of the Fisheries Research Board of Canada*, *25*(8), 1603–1620. https://doi.org/10.1139/f68-145

Adam, P., Schneckenburger, P., Schaeffer, P., & Albrecht, P. (2000). Clues to early diagenetic sulfurization processes from mild chemical cleavage of labile sulfur-rich geomacromolecules. *Geochimica Et Cosmochimica Acta*, *64*, 3485–3503. https://doi.org/10.1016/S0016-7037(00)00443-9

Alleon, J., Bernard, S., Le Guillou, C., Daval, D., Skouri-Panet, F., Kuga, M., & Robert, F. (2017). Organic molecular heterogeneities can withstand diagenesis. *Scientific Reports*, *7*, 1508. https://doi.org/10.1038/s41598-017-01612-8

Allison, P. A. (1986). Soft-bodied animals in the fossil record: The role of decay in fragmentation during transport. *Geology*, *14*, 979–981. https://doi.org/10.1130/0091-7613(1986)14<979:SAITFR>2.0.CO;2

Allison, P. A. (1988a). Konservat-Lagerstatten: Cause and classification. *Paleobiology*, *14*, 331–344. https://doi.org/10.1017/S0094837300012082

Allison, P. A. (1988b). The role of anoxia in the decay and mineralization of proteinaceous macro-fossils. *Paleobiology*, *14*, 139–154. https://doi.org/10.1017/S009483730001188X

Aloulou, F., Kallel, M., Dammak, M., Elleuch, B., & Saliot, A. (2010). Even-numbered n-alkanes/n-alkenes predominance in surface sediments of Gabes Gulf in Tunisia. *Environmental Earth Sciences*, *61*, 1–10. https://doi.org/10.1007/s12665-009-0315-y

Andersen, F. (1996). Fate of organic carbon added as diatom cells to oxic and anoxic marine sediment microcosms. *Marine Ecology Progress Series*, *134*, 225–233. https://doi.org/10.3354/meps134225

Bennike, O. (1997). Quaternary vertebrates from Greenland: A review. *Quaternary Science Reviews*, *16*, 899–909. https://doi.org/10.1016/S0277-3791(97)00002-4

Berner, R. A. (1968a). Rate of concretion growth. *Geochimica Et Cosmochimica Acta*, *32*, 477–483. https://doi.org/10.1016/0016-7037(68)90040-9

Berner, R. A. (1968b). Calcium carbonate concretions formed by the decomposition of organic matter. *Science*, *159*, 195–197. https://doi.org/10.1126/science.159.3811.195

Berner, R. A. (1969). Chemical changes affecting dissolved calcium during the bacterial decomposition of fish and clams in sea water. *Marine Geology*, *7*, 253–274. https://doi.org/10.1016/0025-3227(69)90011-5

Berner, R. A., Scott, M. R., & Thomlinson, C. (1970). Carbonate alkalinity in the pore waters of anoxic marine sediments1: Carbonate alkalinity in sediment pore waters. *Limnology and Oceanography*, *15*, 544–549. https://doi.org/10.4319/lo.1970.15.4.0544

Bianchi, T. S., & Canuel, E. A. (2011). *Chemical biomarkers in aquatic ecosystems*. Princeton University Press.

Blumenberg, M., Thiel, V., & Reitner, J. (2015). Organic matter preservation in the carbonate matrix of a recent microbial mat – Is there a 'mat seal effect'? *Organic Geochemistry*, *87*, 25–34. https://doi.org/10.1016/j.orggeochem.2015.07.005

Bray, E. E., & Evans, E. D. (1961). Distribution of n-paraffins as a clue to recognition of source beds. *Geochimica Et Cosmochimica Acta*, *22*, 2–15. https://doi.org/10.1016/0016-7037(61)90069-2

Briggs, D. E. G. (1995). Experimental taphonomy. *Palaios*, *10*, 539–550. https://doi.org/10.2307/3515093

Briggs, D. E. G. (2003). The role of decay and mineralization in the preservation of soft-bodied fossils. *Annual Review of Earth and Planetary Sciences*, *31*, 275–301. https://doi.org/10.1146/annurev.earth.31.100901.144746

Briggs, D. E. G., & Kear, A. J. (1993). Decay and preservation of polychaetes: Taphonomic thresholds in soft-bodied organisms. *Paleobiology*, *19*, 107–135. https://doi.org/10.1017/S0094837300012343

Briggs, D. E. G., & McMahon, S. (2016). The role of experiments in investigating the taphonomy of exceptional preservation. *Palaeontology*, *59*, 1–11. https://doi.org/10.1111/pala.12219

Briggs, D. E. G., & Summons, R. E. (2014). Ancient biomolecules: Their origins, fossilization, and role in revealing the history of life: Prospects & overviews. *BioEssays*, *36*, 482–490. https://doi.org/10.1002/bies.201400010

Brink, N. W. T. (1975). Holocene history of the Greenland ice sheet based on radiocarbon-dated moraines in West Greenland. *Bulletin Grønlands Geologiske Undersøgelse*, *113*, 1–44. https://doi.org/10.34194/bullggu.v113.6654

Brown, C. M., Henderson, D. M., Vinther, J., Fletcher, I., Sistiaga, A., Herrera, J., & Summons, R. E. (2017). An exceptionally preserved three-dimensional armored dinosaur reveals insights into coloration and cretaceous predator-prey dynamics. *Current Biology*, *27*, 2514–2521.e3. https://doi.org/10.1016/j.cub.2017.06.071

Butler, A. D., Cunningham, J. A., Budd, G. E., & Donoghue, P. C. J. (2015). Experimental taphonomy of Artemia reveals the role of endogenous microbes in mediating decay and fossilization. *Proceedings of the Royal Society B*, *282*, 20150476. https://doi.org/10.1098/rspb.2015.0476

Clements, T., Purnell, M., & Gabbott, S. (2019). The Mazon Creek Lagerstätte: A diverse late Paleozoic ecosystem entombed within siderite concretions. *Journal of the Geological Society*, *176*, 1–11. https://doi.org/10.1144/jgs2018-088

Coleman, M. L. (1993). Microbial processes: Controls on the shape and composition of carbonate concretions. *Marine Geology*, *113*, 127–140. https://doi.org/10.1016/0025-3227(93)90154-N

Coleman, M. L., & Raiswell, R. (1981). Carbon, oxygen and sulphur isotope variations in concretions from the Upper Lias of N.E. England. *Geochimica Et Cosmochimica Acta*, *45*, 329–340. https://doi.org/10.1016/0016-7037(81)90243-X

Coleman, M. L., & Raiswell, R. (1995). Source of carbonate and origin of zonation in pyritiferous carbonate concretions; evaluation of a dynamic model. *American Journal of Science*, *295*, 282–308. https://doi.org/10.2475/ajs.295.3.282

Crisp, M., Demarchi, B., Collins, M., Morgan-Williams, M., Pilgrim, E., & Penkman, K. (2013). Isolation of the intra-crystalline proteins and kinetic studies in *Struthio camelus* (ostrich) eggshell for amino acid geochronology. *Quaternary Geochronology*, *16*, 110–128. https://doi.org/10.1016/j.quageo.2012.09.002

Cronin, T. M., Manley, P. L., Brachfeld, S., Manley, T. O., Willard, D. A., Guilbault, J.-P., Rayburn, J. A., Thunell, R., & Berke, M. (2008). Impacts of post-glacial lake drainage events and revised chronology of the Champlain Sea episode 13–9 ka. *Palaeogeography, Palaeoclimatology, Palaeoecology*, *262*, 46–60. https://doi.org/10.1016/j.palaeo.2008.02.001

Darroch, S. A. F., Laflamme, M., Schiffbauer, J. D., & Briggs, D. E. G. (2012). Experimental formation of a microbial death mask. *Palaios*, *27*, 293–303. https://doi.org/10.2110/palo.2011.p11-059r

Davis, J. B. (1968). Paraffinic hydrocarbons in the sulfate-reducing bacterium *Desulfovibrio desulfuricans*. *Chemical Geology*, *3*, 155–160. https://doi.org/10.1016/0009-2541(68)90007-7

Demarchi, B., Hall, S., Roncal-Herrero, T., Freeman, C. L., Woolley, J., Crisp, M. K., Wilson, J., Fotakis, A., Fischer, R., Kessler, B. M., Rakownikow Jersie-Christensen, R., Olsen, J. V., Haile, J., Thomas, J., Marean, C. W., Parkington, J., Presslee, S., Lee-Thorp, J., Ditchfield, P., … Collins, M. J. (2016). Protein sequences bound to mineral surfaces persist into deep time. *eLife*, *5*, e17092. https://doi.org/10.7554/eLife.17092

Desaulniers, D. E., & Cherry, J. A. (1989a). Origin and movement of groundwater and major ions in a thick deposit of Champlain Sea clay near Montréal. *Canadian Geotechnical Journal*, *26*, 80–89. https://doi.org/10.1139/t89-009

Desaulniers, D. E., & Cherry, J. A. (1989b). Origin and movement of groundwater and major ions in a thick deposit of Champlain Sea clay near Montréal. *Canadian Geotechnical Journal*, *26*, 80–89. https://doi.org/10.1139/t89-009

Dietrich, R., Rülke, A., & Scheinert, M. (2005). Present-day vertical crustal deformations in West Greenland from repeated GPS observations. *Geophysical Journal International*, *163*, 865–874. https://doi.org/10.1111/j.1365-246X.2005.02766.x

Dowling, N. J. E., Widdel, F., & White, D. C. (1986). Phospholipid ester-linked fatty acid biomarkers of acetate-oxidizing sulphate-reducers and other sulphide-forming bacteria. *Microbiology*, *132*, 1815–1825. https://doi.org/10.1099/00221287-132-7-1815

Drenzek, N. J., Montluçon, D. B., Yunker, M. B., Macdonald, R. W., & Eglinton, T. I. (2007). Constraints on the origin of sedimentary organic carbon in the Beaufort Sea from coupled molecular 13C and 14C measurements. *Marine Chemistry*, *103*, 146–162. https://doi.org/10.1016/j.marchem.2006.06.017

Duan, W. M., Hedrick, D. B., Pye, K., Coleman, H. L., & White, D. C. (1996). A preliminary study of the geochemical and microbiological characteristics of modern sedimentary concretions. *Limnology and Oceanography*, *41*, 1404–1414. https://doi.org/10.4319/lo.1996.41.7.1404

Dupraz, C., Reid, R. P., Braissant, O., Decho, A. W., Norman, R. S., & Visscher, P. T. (2009). Processes of carbonate precipitation in modern microbial mats. *Earth-Science Reviews*, *96*, 141–162. https://doi.org/10.1016/j.earscirev.2008.10.005

Edenborn, H. M., Silverberg, N., Mucci, A., & Sundby, B. (1987). Sulfate reduction in deep coastal marine sediments. *Marine Chemistry*, *21*, 329–345. https://doi.org/10.1016/0304-4203(87)90055-7

Eglinton, G., & Hamilton, R. J. (1967). Leaf epicuticular waxes. *Science*, *156*, 1322–1335. https://doi.org/10.1126/science.156.3780.1322

Elder, R. L., & Smith, G. R. (1988). Fish taphonomy and environmental inference in paleolimnology. *Palaeogeography, Palaeoclimatology, Palaeoecology*, *62*, 577–592. https://doi.org/10.1016/0031-0182(88)90072-7

Elvert, M., Boetius, A., Knittel, K., & Jørgensen, B. B. (2003). Characterization of specific membrane fatty acids as chemotaxonomic markers for sulfate-reducing bacteria involved in anaerobic oxidation of methane. *Geomicrobiology Journal*, *20*, 403–419. https://doi.org/10.1080/01490450303894

Fabbri, M., Wiemann, J., Manucci, F., & Briggs, D. E. G. (2020). Three-dimensional soft tissue preservation revealed in the skin of a non-avian dinosaur. *Palaeontology*, *63*, 185–193. https://doi.org/10.1111/pala.12470

Gäb, F., Ballhaus, C., Stinnesbeck, E., Kral, A. G., Janssen, K., & Bierbaum, G. (2020). Experimental taphonomy of fish - role of elevated pressure, salinity and pH. *Scientific Reports*, *10*, 7839. https://doi.org/10.1038/s41598-020-64651-8

Gadd, N. R. (1980). Maximum age for a concretion at Green Creek, Ontario. *Géographie Physique Et Quaternaire*, *34*, 229. https://doi.org/10.7202/1000400ar

Grice, K., Holman, A. I., Plet, C., & Tripp, M. (2019). Fossilised biomolecules and biomarkers in carbonate concretions from Konservat-Lagerstätten. *Minerals*, *9*, 158. https://doi.org/10.3390/min9030158

Grimalt, J., & Albaigés, J. (1987). Sources and occurrence of C12–C22n-alkane distributions with even carbon-number preference in sedimentary environments. *Geochimica Et Cosmochimica Acta*, *51*, 1379–1384. https://doi.org/10.1016/0016-7037(87)90322-X

Gupta, N. S., Cody, G. D., Tetlie, O. E., Briggs, D. E. G., & Summons, R. E. (2009). Rapid incorporation of lipids into macromolecules during experimental decay of invertebrates: Initiation of geopolymer formation. *Organic Geochemistry*, *40*, 589–594. https://doi.org/10.1016/j.orggeochem.2009.02.005

Han, J., & Calvin, M. (1969). Hydrocarbon distribution of algae and bacteria, and microbiological activity in sediments. *Proceedings of the National Academy of Sciences*, *64*, 436–443. https://doi.org/10.1073/pnas.64.2.436

Hebting, Y., Schaeffer, P., Behrens, A., Adam, P., Schmitt, G., Schneckenburger, P., Bernasconi, S. M., & Albrecht, P. (2006). Biomarker evidence for a major preservation pathway of sedimentary organic carbon. *Science*, *312*, 1627–1631. https://doi.org/10.1126/science.1126372

Hedges, J. I., & Keil, R. G. (1995). Sedimentary organic matter preservation: An assessment and speculative synthesis. *Marine Chemistry*, *49*, 81–115. https://doi.org/10.1016/0304-4203(95)00008-F

Henkemans, E., Frape, S. K., Ruskeeniemi, T., Anderson, N. J., & Hobbs, M. (2018). A landscape-isotopic approach to the geochemical characterization of lakes in the Kangerlussuaq region, west Greenland. *Arctic, Antarctic, and Alpine Research*, *50*, S100018. https://doi.org/10.1080/15230430.2017.1420863

Hinrichs, K.-U., Summons, R. E., Orphan, V., Sylva, S. P., & Hayes, J. M. (2000). Molecular and isotopic analysis of anaerobic methane-oxidizing communities in marine sediments. *Organic Geochemistry*, *31*, 1685–1701. https://doi.org/10.1016/S0146-6380(00)00106-6

Holman, J. A., Harington, C. R., & Mott, R. J. (1997). Skeleton of a leopard frog (*Rana pipiens*) from Champlain Sea deposits (ca. 10,000 BP) near Eardley, Quebec. *Canadian Journal of Earth Sciences*, *34*, 1150–1155. https://doi.org/10.1139/e17-092

Hotelling, H. (1933). Analysis of a complex of statistical variables into principal components. *Journal of Educational Psychology*, *24*, 417. https://doi.org/10.1037/h0071325

Ingalls, A. E., Aller, R. C., Lee, C., & Wakeham, S. G. (2004). Organic matter diagenesis in shallow water carbonate sediments. *Geochimica Et Cosmochimica Acta*, *68*, 4363–4379. https://doi.org/10.1016/j.gca.2004.01.002

Iniesto, M., Laguna, C., Florín, M., Guerrero, M. C., Chicote, A., Buscalioni, A. D., & López-Archilla, A. I. (2015). The impact of microbial mats and their microenvironmental conditions in early decay of fish. *Palaios*, *30*, 792–801. https://doi.org/10.2110/palo.2014.086

Iniesto, M., Lopez-Archilla, A. I., Fregenal-Martinez, M., Buscalioni, A. D., & Guerrero, M. C. (2013). Involvement of microbial mats in delayed decay: An experimental essay on fish preservation. *Palaios*, *28*, 56–66. https://doi.org/10.2110/palo.2011.p11-099r

Iniesto, M., Villalba, I., Buscalioni, A. D., Guerrero, M. C., & López-Archilla, A. I. (2017). The effect of microbial mats in the decay of anurans with implications for understanding taphonomic processes in the fossil record. *Scientific Reports*, *7*, 45160. https://doi.org/10.1038/srep45160

Jørgensen, B. B., Postgate, J. R., Postgate, J. R., & Kelly, D. P. (1982). Ecology of the bacteria of the sulphur cycle with special reference to anoxic—oxic interface environments. *Philosophical Transactions of the Royal Society of London. B, Biological Sciences*, *298*, 543–561. https://doi.org/10.1098/rstb.1982.0096

Kempe, S., & Kazmierczak, J. (1994). The role of alkalinity in the evolution of ocean chemistry, organization of living systems, and biocalcification processes. *Bulletin De La Institut Océanographique (Monaco)*, *13*, 61–117.

Larter, S. R., & Douglas, A. G. (1980). Melanoidins—kerogen precursors and geochemical lipid sinks: A study using pyrolysis gas chromatography (PGC). *Geochimica Et Cosmochimica Acta*, *44*, 2087–2095. https://doi.org/10.1016/0016-7037(80)90206-9

Lehmann, M. F., Bernasconi, S. M., Barbieri, A., & McKenzie, J. A. (2002). Preservation of organic matter and alteration of its carbon and nitrogen isotope composition during simulated and in situ early sedimentary diagenesis. *Geochimica Et Cosmochimica Acta*, *66*, 3573–3584. https://doi.org/10.1016/S0016-7037(02)00968-7

Lengger, S. K., Melendez, I. M., Summons, R. E., & Grice, K. (2017). Mudstones and embedded concretions show differences in lithology-related, but not source-related biomarker distributions. *Organic Geochemistry*, *113*, 67–74. https://doi.org/10.1016/j.orggeochem.2017.08.003

Lindgren, J., Uvdal, P., Sjövall, P., Nilsson, D. E., Engdahl, A., Schultz, B. P., & Thiel, V. (2012). Molecular preservation of the pigment melanin in fossil melanosomes. *Nature Communications*, *3*, 824. https://doi.org/10.1038/ncomms1819

McAllister, D. E., Cumbaa, S. L., & Harington, C. R. (1981). Pleistocene fishes (Coregonus, Osmerus, Microgadus, Gasterosteus) from Green Creek, Ontario, Canada. *Canadian Journal of Earth Sciences*, *18*, 1356–1364. https://doi.org/10.1139/e81-125

Mcbride, E. F., & Milliken, K. L. (2006). Giant calcite-cemented concretions, Dakota Formation, central Kansas, USA: Giant concretions in Dakota Sandstone, Kansas, USA. *Sedimentology*, *53*, 1161–1179. https://doi.org/10.1111/j.1365-3091.2006.00813.x

McCoy, V. E., Wiemann, J., Lamsdell, J. C., Whalen, C. D., Lidgard, S., Mayer, P., Petermann, H., & Briggs, D. E. G. (2020). Chemical signatures of soft tissues distinguish between vertebrates and invertebrates from the Carboniferous Mazon Creek Lagerstätte of Illinois. *Geobiology*, *18*, 560–565. https://doi.org/10.1111/gbi.12397

McCoy, V. E., Young, R. T., & Briggs, D. E. G. (2015a). Sediment permeability and the preservation of soft-tissues in concretions: An experimental study. *Palaios*, *30*, 608–612. https://doi.org/10.2110/palo.2015.002

McCoy, V. E., Young, R. T., & Briggs, D. E. G. (2015b). Factors controlling exceptional preservation in concretions. *Palaios*, *30*, 272–280. https://doi.org/10.2110/palo.2014.081

McKirdy, D. M., Thorpe, C. S., Haynes, D. E., Grice, K., Krull, E. S., Halverson, G. P., & Webster, L. J. (2010). The biogeochemical evolution of the Coorong during the mid- to late Holocene: An elemental, isotopic and biomarker perspective. *Organic Geochemistry*, *41*(2), 96–110. https://doi.org/10.1016/j.orggeochem.2009.07.010

Mcnamara, M. E., Orr, P. J., Kearns, S. L., Alcala, L., Anadon, P., & Penalver Molla, E. (2009). Soft-tissue preservation in miocene frogs from Libros, Spain: Insights into the genesis of decay microenvironments. *Palaios*, *24*, 104–117. https://doi.org/10.2110/palo.2008.p08-017r

Melendez, I., Grice, K., & Schwark, L. (2013). Exceptional preservation of Palaeozoic steroids in a diagenetic continuum. *Scientific Reports*, *3*, 1–6. https://doi.org/10.1038/srep02768

Melendez, I., Grice, K., Trinajstic, K., Ladjavardi, M., Greenwood, P., & Thompson, K. (2013). Biomarkers reveal the role of photic zone euxinia in exceptional fossil preservation: An organic geochemical perspective. *Geology*, *41*, 123–126. https://doi.org/10.1130/G33492.1

Meyers, P. A. (1997). Organic geochemical proxies of paleoceanographic, paleolimnologic, and paleoclimatic processes. *Organic Geochemistry*, *27*, 213–250. https://doi.org/10.1016/S0146-6380(97)00049-1

Mojarro, A., Uveges, B., Roberts, M., Vinther, J., & Summons, R. E. (2021). Preliminary ams 14C measurements from holocene-age carbonate concretions. In: *30th international meeting on organic geochemistry* (pp. 1–2). European Association of Geoscientists & Engineers. https://doi.org/10.3997/2214-4609.202134227

Mozley, P. S. (1996). The internal structure of carbonate concretions in mudrocks: A critical evaluation of the conventional concentric model of concretion growth. *Sedimentary Geology*, *103*, 85–91. https://doi.org/10.1016/0037-0738(95)00087-9

Muscente, A. D., Schiffbauer, J. D., Broce, J., Laflamme, M., O'Donnell, K., Boag, T. H., Meyer, M., Hawkins, A. D., Huntley, J. W., McNamara, M., MacKenzie, L. A., Stanley, G. D., Hinman, N. W., Hofmann, M. H., & Xiao, S. (2017). Exceptionally preserved fossil assemblages through geologic time and space. *Gondwana Research*, *48*, 164–188. https://doi.org/10.1016/j.gr.2017.04.020

Naimark, E., Kalinina, M., Shokurov, A., Boeva, N., Markov, A., & Zaytseva, L. (2016). Decaying in different clays: Implications for soft-tissue preservation. *Palaeontology*, *59*, 583–595. https://doi.org/10.1111/pala.12246

Nakashima, B. (2002). Capelin (*Mallotus villosus*) spawning behaviour in Newfoundland waters – The interaction between beach and demersal spawning. *ICES Journal of Marine Science*, *59*, 909–916. https://doi.org/10.1006/jmsc.2002.1261

Nishimura, M., & Baker, E. W. (1986). Possible origin of n-alkanes with a remarkable even-to-odd predominance in recent marine sediments. *Geochimica Et Cosmochimica Acta*, *50*, 299–305. https://doi.org/10.1016/0016-7037(86)90178-X

O'Reilly, S. S., Mariotti, G., Winter, A. R., Newman, S. A., Matys, E. D., McDermott, F., Pruss, S. B., Bosak, T., Summons, R. E., & Klepac-Ceraj, V. (2017). Molecular biosignatures reveal common benthic microbial sources of organic matter in ooids and grapestones from Pigeon Cay, The Bahamas. *Geobiology*, *15*, 112–130. https://doi.org/10.1111/gbi.12196

Oskam, C. L., Haile, J., McLay, E., Rigby, P., Allentoft, M. E., Olsen, M. E., Bengtsson, C., Miller, G. H., Schwenninger, J.-L., Jacomb, C., Walter, R., Baynes, A., Dortch, J., Parker-Pearson, M., Gilbert, M. T. P., Holdaway, R. N., Willerslev, E., & Bunce, M. (2010). Fossil avian eggshell preserves ancient DNA. *Proceedings of the Royal Society B*, *277*, 1991–2000. https://doi.org/10.1098/rspb.2009.2019

Parent, M., & Occhietti, S. (1988). Late Wisconsinan deglaciation and Champlain Sea invasion in the St. Lawrence Valley, Québec. *Géographie Physique Et Quaternaire*, *42*, 215. https://doi.org/10.7202/032734ar

Parry, L. A., Smithwick, F., Nordén, K. K., Saitta, E. T., Lozano-Fernandez, J., Tanner, A. R., Caron, J.-B., Edgecombe, G. D., Briggs, D. E. G., & Vinther, J. (2018). Soft-bodied fossils are not simply rotten carcasses - Toward a holistic understanding of exceptional fossil preservation: Exceptional fossil preservation is complex and involves the interplay of numerous biological and geological processes. *BioEssays*, *40*, 1700167. https://doi.org/10.1002/bies.201700167

Plet, C., Grice, K., Pagès, A., Verrall, M., Coolen, M. J. L., Ruebsam, W., Rickard, W. D. A., & Schwark, L. (2017). Palaeobiology of red and white blood cell-like structures, collagen and cholesterol in an ichthyosaur bone. *Scientific Reports*, *7*, 13776. https://doi.org/10.1038/s41598-017-13873-4

Prost, K., Birk, J. J., Lehndorff, E., Gerlach, R., & Amelung, W. (2017). Steroid biomarkers revisited – Improved source identification of faecal remains in archaeological soil material. *PLoS One*, *12*, e0164882. https://doi.org/10.1371/journal.pone.0164882

Purnell, M. A., Donoghue, P. J. C., Gabbott, S. E., McNamara, M. E., Murdock, D. J. E., & Sansom, R. S. (2018). Experimental analysis of soft-tissue fossilization: Opening the black box. *Palaeontology*, *61*, 317–323. https://doi.org/10.1111/pala.12360

Pye, K., Dickson, J. A. D., Schiavon, N., Coleman, M. L., & Cox, M. (1990). Formation of siderite-Mg-calcite-iron sulphide concretions in intertidal marsh and sandflat sediments, north Norfolk, England. *Sedimentology*, *37*, 325–343. https://doi.org/10.1111/j.1365-3091.1990.tb00962.x

Raiswell, R. (1976). The microbiological formation of carbonate concretions in the Upper Lias of NE England. *Chemical Geology*, *18*, 227–244. https://doi.org/10.1016/0009-2541(76)90006-1

Raiswell, R., & Fisher, Q. J. (2000). Mudrock-hosted carbonate concretions: A review of growth mechanisms and their influence on chemical and isotopic composition. *Journal of the Geological Society*, *157*, 239–251. https://doi.org/10.1144/jgs.157.1.239

Ran-Ressler, R. R., Lawrence, P., & Brenna, J. T. (2012). Structural characterization of saturated branched chain fatty acid methyl esters by collisional dissociation of molecular ions generated by electron ionization. *Journal of Lipid Research*, *53*, 195–203. https://doi.org/10.1194/jlr.D020651

Řezanka, T. (1989). Very-long-chain fatty acids from the animal and plant kingdoms. *Progress in Lipid Research*, *28*, 147–187. https://doi.org/10.1016/0163-7827(89)90011-8

Řezanka, T., Sokolov, M. Y., & Víden, I. (1990). Unusual and very-long-chain fatty acids in Desulfotomaculum, a sulfate-reducing bacterium. *FEMS Microbiology Letters*, *73*, 231–237.

Rielley, G., Collier, R. J., Jones, D. M., & Eglinton, G. (1991). The biogeochemistry of Ellesmere Lake, U.K.—I: Source correlation of leaf wax inputs to the sedimentary lipid record. *Organic Geochemistry*, *17*, 901–912. https://doi.org/10.1016/0146-6380(91)90031-E

Sagemann, J., Bale, S. J., Briggs, D. E. G., & Parkes, R. J. (1999). Controls on the formation of authigenic minerals in association with decaying organic matter: An experimental approach. *Geochimica Et Cosmochimica Acta*, *63*, 1083–1095. https://doi.org/10.1016/S0016-7037(99)00087-3

Sand, K. K., Pedersen, C. S., Sjöberg, S., Nielsen, J. W., Makovicky, E., & Stipp, S. L. S. (2014). Biomineralization: Long-term effectiveness of polysaccharides on the growth and dissolution of calcite. *Crystal Growth & Design*, *14*, 5486–5494. https://doi.org/10.1021/cg5006743

Sansom, R. S. (2014). Experimental decay of soft tissues. *The Paleontological Society Papers*, *20*, 259–274. https://doi.org/10.1017/S1089332600002886

Sansom, R. S., Gabbott, S. E., & Purnell, M. A. (2011). Decay of vertebrate characters in hagfish and lamprey (Cyclostomata) and the implications for the vertebrate fossil record. *Proceedings of the Royal Society B*, *278*, 1150–1157. https://doi.org/10.1098/rspb.2010.1641

Seilacher, A. (2001). Concretion morphologies reflecting diagenetic and epigenetic pathways. *Sedimentary Geology*, *143*, 41–57. https://doi.org/10.1016/S0037-0738(01)00092-6

Sigurgisladóttir, S., & Pálmadóttir, H. (1993). Fatty acid composition of thirty-five Icelandic fish species. *Journal of the American Oil Chemists Society*, *70*, 1081–1087. https://doi.org/10.1007/BF02632146

Sinninghe Damsté, J. S., Irene, W., Rijpstra, C., de Leeuw, J. W., & Schenck, P. A. (1988). Origin of organic sulphur compounds and sulphur-containing high molecular weight substances in sediments and immature crude oils. *Organic Geochemistry*, *13*, 593–606. https://doi.org/10.1016/0146-6380(88)90079-4

Smittenberg, R. H., Pancost, R. D., Hopmans, E. C., Paetzel, M., & Sinninghe Damsté, J. S. (2004). A 400-year record of environmental change in an euxinic fjord as revealed by the sedimentary biomarker record. *Palaeogeography, Palaeoclimatology, Palaeoecology*, *202*, 331–351. https://doi.org/10.1016/S0031-0182(03)00642-4

Soldal, O., Mauring, E., Halvorsen, E., & Rye, N. (1994). Seawater intrusion and fresh groundwater hydraulics in fjord delta aquifers inferred from ground penetrating radar and resistivity profiles—Sunndalsøra and Esebotn, western Norway. *Journal of Applied Geophysics*, *32*, 305–319. https://doi.org/10.1016/0926-9851(94)90030-2

Soldal, O., & Rye, N. (1995). Hydrogeology of a fjord delta aquifer, Sunndalsøra, Norway. *Norsk Geologisk Tidsskrift*, *75*, 169–178.

Storms, J. E. A., de Winter, I. L., Overeem, I., Drijkoningen, G. G., & Lykke-Andersen, H. (2012). The Holocene sedimentary history of

the Kangerlussuaq Fjord-valley fill, West Greenland. *Quaternary Science Reviews*, *35*, 29–50. https://doi.org/10.1016/j.quascirev.2011.12.014

Summons, R. E., Bird, L. R., Gillespie, A. L., Pruss, S. B., Roberts, M., & Sessions, A. L. (2013). Lipid biomarkers in ooids from different locations and ages: Evidence for a common bacterial flora. *Geobiology*, *11*, 420–436. https://doi.org/10.1111/gbi.12047

Sun, M., Wakeham, S. G., & Lee, C. (1997). Rates and mechanisms of fatty acid degradation in oxic and anoxic coastal marine sediments of Long Island Sound, New York, USA. *Geochimica Et Cosmochimica Acta*, *61*, 341–355. https://doi.org/10.1016/S0016-7037(96)00315-8

Taylor, J., & Parkes, R. J. (1983). The cellular fatty acids of the sulphate-reducing bacteria, *Desulfobacter* sp. *Desulfobulbus* sp. and *Desulfovibrio desulfuricans*. *Microbiology*, *129*, 3303–3309. https://doi.org/10.1099/00221287-129-11-3303

Thiel, V., & Hoppert, M. (2018). Fatty acids and other biomarkers in two Early Jurassic concretions and their immediate host rocks (Lias δ, Buttenheim clay pit, Bavaria, Germany). *Organic Geochemistry*, *120*, 42–55. https://doi.org/10.1016/j.orggeochem.2018.02.010

Volkman, J. K. (2006). Lipid markers for marine organic matter. In J. K. Volkman (Ed.), *Marine organic matter: Biomarkers, isotopes and DNA* (pp. 27–70). Springer-Verlag. https://doi.org/10.1007/698_2_002

Volkman, J. K., Barrett, S. M., Blackburn, S. I., Mansour, M. P., Sikes, E. L., & Gelin, F. (1998). Microalgal biomarkers: A review of recent research developments. *Organic Geochemistry*, *29*, 1163–1179. https://doi.org/10.1016/S0146-6380(98)00062-X

Volkman, J. K., Johns, R. B., Gillan, F. T., Perry, G. J., & Bavor, H. J. (1980). Microbial lipids of an intertidal sediment—I. Fatty acids and hydrocarbons. *Geochimica Et Cosmochimica Acta*, *44*, 1133–1143. https://doi.org/10.1016/0016-7037(80)90067-8

Wiemann, J., Crawford, J. M., & Briggs, D. E. G. (2020). Phylogenetic and physiological signals in metazoan fossil biomolecules. *Science Advances*, *6*, eaba6883. https://doi.org/10.1126/sciadv.aba6883

Wiemann, J., Fabbri, M., Yang, T.-R., Stein, K., Sander, P. M., Norell, M. A., & Briggs, D. E. G. (2018). Fossilization transforms vertebrate hard tissue proteins into N-heterocyclic polymers. *Nature Communications*, *9*, 4741. https://doi.org/10.1038/s41467-018-07013-3

Wilson, D., & Brett, C. (2013). Concretions as sources of exceptional preservation, and decay as a source of concretions: Examples from the middle Devonian of New York. *Palaios*, *28*, 305–316. https://doi.org/10.2110/palo.2012.p12-086r

Zatoń, M., & Marynowski, L. (2004). Konzentrat-Lagerstätte-type carbonate concretions from the uppermost Bajocian (Middle Jurassic) of the Częstochowa area, South-Cental Poland. *Geological Quarterly*, *48*, 339–350.

SUPPORTING INFORMATION

Additional supporting information may be found in the online version of the article at the publisher's website.

How to cite this article: Mojarro, A., Cui, X., Zhang, X., Jost, A. B., Bergmann, K. D., Vinther, J., & Summons, R. E. (2022). Comparative soft-tissue preservation in Holocene-age capelin concretions. *Geobiology*, 20, 377–398. https://doi.org/10.1111/gbi.12480